Neonatal brain dynamic functional connectivity: impact of preterm birth and association with early childhood neurodevelopment

Lucas G. S. França[1,2], Judit Ciarrusta[1,2], Oliver Gale-Grant[1,2], Sunniva Fenn-Moltu[1,2], Sean Fitzgibbon[3], Andrew Chew[2], Shona Falconer[2], Ralica Dimitrova[1,2], Lucilio Cordero-Grande[2,4,5], Anthony N Price[2], Emer Hughes[2], Jonathan O'Muircheartaigh[1,2,6], Eugene Duff[3], Jetro J Tuulari[7,8,9], Gustavo Deco[10,11,12,13], Serena J Counsell[2], Chiara Nosarti[2,14], Tomoki Arichi[2,6,15,16], A David Edwards[2,6*], Grainne McAlonan[1*], Dafnis Batalle[1,2*†]

1) Department of Forensic and Neurodevelopmental Science, Institute of Psychiatry, Psychology & Neuroscience, King's College London, London SE5 8AF, United Kingdom

2) Centre for the Developing Brain, School of Biomedical Engineering & Imaging Sciences, King's College London, London SE1 7EH, United Kingdom

3) Oxford Centre for Functional Magnetic Resonance Imaging of the Brain, Wellcome Centre for Integrative Neuroimaging, University of Oxford, Oxford OX3 9DU, United Kingdom

4) Biomedical Image Technologies, Higher Technical School of Engineers in Telecommunication, Polytechnic University of Madrid, 28040 Madrid, Spain

5) Center for Biomedical Research Network – Bioengineering, Biomaterials and Nanomedicine, Carlos III Health Institute, 28029 Madrid, Spain

6) MRC Centre for Neurodevelopmental Disorders, King's College London, London SE1 1UL, United Kingdom

7) FinnBrain Birth Cohort Study, Turku Brain and Mind Center, Institute of Clinical Medicine, University of Turku, 20500 Turku, Finland

8) Turku Collegium for Science and Medicine and Technology, University of Turku, 20500 Turku, Finland

9) Department of Psychiatry, University of Turku and Turku University Hospital, 20500 Turku, Finland

10) Center for Brain and Cognition, Computational Neuroscience Group, Department of Information and Communication Technologies, Pompeu Fabra University, 08002, Barcelona, Spain

11) Catalan Institution for Research and Advanced Studies, 08010 Barcelona, Spain

12) Department of Neuropsychology, Max Planck Institute for Human Cognitive and Brain Sciences, 04103 Leipzig, Germany

13) School of Psychological Sciences, Monash University, Melbourne VIC 3010, Australia

14) Department of Child and Adolescent Psychiatry, Institute of Psychiatry, Psychology & Neuroscience, King's College London, London SE5 8AF, United Kingdom

15) Department of Paediatric Neurosciences, Evelina London Children's Hospital, Guy's and St Thomas' NHS Foundation Trust, London SE1 7EH, United Kingdom

16) Department of Bioengineering, Imperial College London, London SW7 2AZ, United Kingdom

***Joint senior authors**

†Corresponding author:
Dafnis Batalle
Main IoPPN Building, Office E1.22 (1st Floor, FANS)
16, De Crespigny Park, SE5 8AF, London, UK
dafnis.batalle@kcl.ac.uk

Running title: Neonatal dynamic functional connectivity

Abstract

Brain functional dynamics have been linked to emotion and cognition in mature individuals, where alterations are associated with mental ill-health and neurodevelopmental conditions (such as autism spectrum disorder). Although reliable resting-state networks have been consistently identified in neonates, little is known about the early development of dynamic brain functional connectivity and whether it is linked to later neurodevelopmental outcomes in childhood. In this study we characterised dynamic functional connectivity in the first few weeks of postnatal life and evaluated whether early dynamic functional connectivity: i) changes with age in the neonatal period ii) is altered by preterm birth and iii) is associated with neurodevelopmental and behavioural outcomes at 18 months.

We used the Kuramoto Order Parameter as a metric of global brain synchrony and defined transient brain states (modules) using Leading Eigenvector Analysis (LEiDA) in a cohort of term-born (n=324) and preterm-born babies (n=66) scanned at term equivalent age from the developing Human Connectome Project. We assessed whether neonatal brain state features (mean synchrony, metastability, entropy, fractional occupancy, dwelling times) and state transition probabilities were associated with postmenstrual age at scan , postnatal days at scan and preterm-birth; and correlate with neurodevelopmental outcomes at 18 months measured using the Bayley Scales of Infant and Toddler Development, and atypical social, sensory and repetitive behaviours measured by the Quantitative Checklist for Autism in Toddlers (Q-CHAT).

On a global scale, preterm-born infants had lower mean synchronisation and metastability, with reduced mean synchronisation associated with higher Q-CHAT scores at 18 months of age. On a modular scale, we identified six transient states of neonatal dynamic functional connectivity: three whole-brain synchronisation states and three regional synchrony states occupying occipital, sensory-motor, and frontal regions. Mean synchrony, metastability, fractional occupancy and dwelling times of these brain states were correlated with postmenstrual age and postnatal days at scan. Preterm-born infants had increased fractional occupancy of frontal and occipital states. Higher neonatal sensory-motor synchronisation was associated with lower motor and language outcome scores at 18 months. Lower frequency of occurrence of whole-brain synchronisation states and higher frequency of occurrence of the sensory-motor state were associated with higher Q-CHAT scores at 18 months.

Thus, we have shown for the first time that a dynamic landscape of brain connectivity is already established by the time of birth in the human brain. This landscape is altered by preterm birth and its profile is linked to neurodevelopmental outcomes in toddlerhood.

1. Introduction

A fundamental feature of the brain's activity is the dynamic properties of its functional connectivity, with continuous shifting between different connectivity profiles or 'states'. These dynamic properties are linked to processes such as language (Chyl et al., 2021; Erb et al., 2013), cognition (Allen et al., 2014; Calhoun et al., 2014; Díez-Cirarda et al., 2018; Gonzalez-Castillo and Bandettini, 2018; Hellyer et al., 2015, 2014; Hutchison et al., 2013; Lurie et al., 2020; Ponce-Alvarez et al., 2015, p.; Schaefer et al., 2014; Tagliazucchi and Laufs, 2014), and motor function (Engels et al., 2018; Wang et al., 2010). Importantly, altered brain dynamics have also been linked to the clinical features and/or cognitive dysfunction in neurodevelopmental conditions such as schizophrenia (Sakoğlu et al., 2010), attention deficit hyperactivity disorder (ADHD)(de Lacy and Calhoun, 2019) and autism spectrum disorder (ASD) (de Lacy et al., 2017; Watanabe and Rees, 2017). Individuals with ASD, for example, have been reported to switch between different connectivity profiles more directly, whereas typically developing individuals switch between those same brain states via an intermediate connectivity profile (Watanabe and Rees, 2017). However, although it is increasingly appreciated that neurodevelopmental conditions likely have their origins in the perinatal period, little is known about the brain's dynamic properties at this critical juncture. Moreover, it is also not clear whether its dynamic characteristics are associated with later childhood neurodevelopment, and in particular, which of these characteristics signal a higher likelihood of later neurodevelopmental difficulties.

Conventional studies of "static" functional brain connectivity in early life have shown that the spatial representation of resting state networks (RSNs) appears to be relatively mature and adult-like even soon after birth (Doria et al., 2010; Fransson et al., 2009, 2007; Smyser et al., 2016, 2010). It has also been confirmed that these RSNs may be disrupted by perinatal exposures, such as preterm birth (Doria et al., 2010; Eyre et al., 2021; Gao et al., 2015a, 2015b; Smyser et al., 2016, 2010), which increase the likelihood of neurodevelopmental impairments (Boardman and Counsell, 2020). However, despite the evidence for the importance of dynamics in older groups, the dynamics of these networks in early life remain unexplored.

In this study we applied state-of-the-art techniques to evaluate functional Magnetic Resonance Imaging (fMRI) acquired as part of the developing Human Connectome Project (dHCP), the largest publicly available population-based dataset of the healthy new-born brain (Edwards et al., 2022). We used two methods that tap into dynamic brain function. First, we characterised global dynamics - which are aggregates of the level of synchronisation across different areas of the brain – using Kuramoto Order Parameter (KOP) based measures, namely mean synchronisation and metastability. Second, we characterised modular dynamics. That is, we identified networks and sub-networks involved in temporal 'states', i.e., paroxysmal modes representing synchronisation of the brain, using Leading Eigenvector Analysis (LEiDA) (Cabral et al., 2017; Figueroa et al., 2019; Lord et al., 2019; Vohryzek et al., 2020). This allowed us to test three hypotheses: 1) That neonatal brain dynamics quickly develop with age at scan; 2) That preterm birth alters the typical pattern of functional brain dynamics; and 3) That neonatal brain dynamics are linked to neurodevelopmental and behavioural outcome measures at age 18 months.

2. Methods

2.1. Participants

We analysed a total of 390 (out of 809) datasets from the dHCP (release 3) (Edwards et al., 2022) acquired from both term (n = 324) and preterm born (gestational age (GA) at birth < 37 weeks; n = 66) babies. Full inclusion and exclusion criteria and numbers excluded at each step are detailed in Supplementary Figure S1. Term-born babies were born at median GA at birth of 40.14 weeks (IQR = 1.86 weeks) and scanned soon after birth (median postmenstrual age (PMA) at scan = 41.57, IQR = 2.43 weeks). Preterm-born babies were born at a median GA at birth of 33.36 weeks (IQR = 5.86 weeks) and scanned at term-equivalent age (median PMA at scan = 40.5 (IQR = 2.71)). Table 1 shows demographic data of the sample. The distribution of PMA at scan and GA at birth for the individuals included in this study is shown in Supplementary Figure S2. All children were invited to the Centre for the Developing Brain, St Thomas' Hospital, London, for neurodevelopmental evaluation by experienced paediatricians or psychologists at 18 months after expected delivery date. The Bayley Scales of Infant and Toddler Development, Third Edition (BSID-III) (Bayley, 2006) were used to assess general developmental outcomes across motor, language and cognitive domains in 305 individuals from the total population, comprising 257 infants born at term and 48 born preterm (higher scores indicate greater skills). Of these, the Quantitative Checklist for Autism in Toddlers (Q-CHAT) (Allison et al., 2008) at 18 months corrected age was available in 300 individuals (254 born at term and 46 born preterm), as a measure of atypical social, sensory and repetitive behaviours which occur as a continuum in the population (Allison et al., 2008). Although higher Q-CHAT scores may indicate more threshold or subthreshold autistic traits, we emphasize our use of this instrument was to capture behaviours not tapped by the BSID-III, rather than to screen for ASD. The index of multiple deprivation (IMD) rank – a composite measure of geographical deprivation estimated from the address of the mother at the time of birth (Abel et al., 2016) – was obtained for every subject and included as a covariate for models aimed at assessing the relationship between neonatal brain dynamics and subsequent neurodevelopmental and behavioural outcomes.

2.2. MRI data acquisition

We evaluated fMRI acquisitions obtained as part of the dHCP at the Evelina Newborn Imaging Centre, Evelina London Children's Hospital, using a 3 Tesla Philips Achieva system (Philips Medical Systems). Ethical approval was given by the UK National Research Ethics Authority (14/LO/1169), and written consent was obtained from all participating families prior to data collection. Scans were performed without sedation in a dedicated neonatal set-up with optimised transport system, positioning devices, hearing protection, and custom-built 32-channel receive head coil and acoustic hood (Hughes et al., 2017). Scans were supervised by a neonatal nurse or paediatrician who monitored heart rate, oxygen saturation and temperature throughout the duration of the scan. Blood-oxygen-level-dependent (BOLD) fMRI was acquired using a multi-slice echo planar imaging sequence with multiband excitation (factor 9) (repetition time (TR) = 392 ms, echo time (TE) = 38 ms, voxel size = 2.15 x 2.15 x 2.15 mm, flip angle = 34°, 45 slices, total time = 15 m 3 s, number of volumes = 2300) (Edwards et al.,

2022). Anatomical images were acquired for brain morphometry and clinical reporting (Edwards et al., 2022). T1-weighted images had a reconstructed spatial resolution = 0.8 x 0.8 x 0.8 mm, field of view = 145 x 122 x 100 mm, TR = 4795 ms. T2-weighted images had a reconstructed spatial resolution = 0.8 x 0.8 x 0.8 mm, field of view = 145 x 145 x 108 mm, TR = 12 s, TE = 156 ms. fMRI datasets with excessive motion (more than 10% of motion outliers (Eyre et al., 2021)), or incidental MRI findings of clinical significance (radiology scores 4 or 5 which indicate major lesions within white matter, cortex, basal ganglia or cerebellum – as described in dHCP database (Edwards et al., 2022)) were excluded. In cases of twin/triplet scans only one infant was included (the one with least motion outliers during acquisition).

Table 1 Demographic details of the term- and preterm-born groups.

	Term (n = 324)	Preterm (n = 66)	Statistic	p-value
Demographics & Clinical Details				
GA at birth [in weeks] (S.D.)	40.04 (1.26)	32.79 (3.40)	12.814[a]	$p < 0.001$
PMA at scan [in weeks] (S.D.)	41.60 (1.67)	40.60 (2.13)	3.615[a]	$p < 0.001$
Sex [female count] (%)	149 (45.99)	26 (39.39)	0.716[b]	$p = 0.398$
% FD outliers (S.D.)	5.38 (2.62)	4.52 (2.49)	2.451[a]	$p = 0.014$
Follow-up				
Corrected age at follow-up[†] [months] (S.D.)	18.83 (1.30)	18.71 (1.35)	0.672[a]	*$p = 0.503$*
Uncorrected age at follow-up[†] [months] (S.D.)	18.82 (1.34)	20.40 (1.45)	-7.060[a]	$p < 0.001$
Bayley III[†] - cognitive (S.D.)	101.56 (10.70)	99.90 (13.11)	0.618[a]	$p = 0.538$
Bayley III[†] - motor (S.D.)	102.25 (9.72)	99.65 (10.26)	1.733[a]	$p = 0.083$
Bayley III[†] - language (S.D.)	99.33 (15.72)	95.69 (15.85)	1.155[a]	$p = 0.249$
Q-CHAT[††] (S.D.)	29.90 (8.51)	31.63 (11.81)	-0.682[a]	$p = 0.497$

[†]Bayley Scales of Infant Development: Third Edition - # of complete assessments: 257 term, 48 preterm
[††]Quantitative Checklist for Autism in Toddlers - # of complete assessments: 254 term, 46 preterm
[a]Z (Mann-Whitney U-test), [b]χ^2-test
FD – Framewise Displacement

2.3. Data processing

Individual fMRI datasets were pre-processed according to the dHCP dedicated neonatal pipeline (Fitzgibbon et al., 2020). Briefly, local distortion due to field inhomogeneity was corrected using *topup* (Andersson et al., 2003); intra- and inter-volume motion correction; and associated dynamic distortions correction using rigid-body realignment and slice-to-volume *eddy* (Andersson et al., 2017; Andersson and Sotiropoulos, 2016). Residual motion, multiband acquisition, and cardiorespiratory artefacts were regressed out using FSL FIX (Griffanti et al., 2014; Salimi-Khorshidi et al., 2014).

Head motion has been shown to produce spurious and systematic correlations in resting state fMRI (Power et al., 2012). In addition to specific processing steps within the dHCP pipeline implemented to minimise motion artifact on the BOLD signal (Fitzgibbon et al., 2020), we also evaluated motion magnitude for each dataset using framewise displacement (FD) (Power et al.,

2014, 2012). To minimise the effects of motion (and/or any likely associated differences) on the determination of brain states, only participants with less than 10% motion outliers (defined as FD > 75th centile + 1.5*IQR) were selected for the final analysed subsample. The total number of motion outliers was additionally used as a covariate of control in the analysis models described in the statistics section.

We performed a segmentation of the T2-weighted volumes with a dedicated neonatal tissue segmentation pipeline (Makropoulos et al., 2014). We parcellated each subject's T2-weighted volume in 90 cortical and subcortical parcels using the Anatomical Automated Labels (AAL) atlas (Tzourio-Mazoyer et al., 2002), mapped to the neonatal brain (Shi et al., 2011), adapted and manually corrected into the dHCP high-resolution template (Schuh et al., 2018). We transformed the AAL atlas into each subject's native space with a non-linear registration based on a diffeomorphic symmetric image normalisation method (SyN) (Avants et al., 2011) using T2-weighted contrast and the segmentation obtained previously. Grey matter segmentation and parcels were propagated from T2 native space into each subject's fMRI space with a boundary-based linear registration available as part of the functional dHCP processing pipeline (Fitzgibbon et al., 2020). Average BOLD timeseries were then calculated for each of the 90 AAL parcels in their intersection with grey matter, deep grey matter, and basal ganglia segmentation masks.

2.4. Analysing BOLD timeseries

We filtered the BOLD timeseries with a bandpass Butterworth second order filter in the range of 0.02-0.10 Hz (Lord et al., 2019) and obtained the phases $\varphi_j(t)$ for each parcel in time with the Hilbert transform. For a given real signal $s(t)$, we built a complex signal *z(t)* (Boashash, 1992; Glerean et al., 2012) given by:

$$z(t) = s(t) + iH[s(t)] \quad (1)$$

In which $H[s(t)]$ represented a Hilbert transform applied to the real signal s(t) and is defined below, with p.v. consisting of Cauchy principle value (Boashash, 1992):

$$H[s(t)] = p.v. \int_{-\infty}^{\infty} \frac{s(t-\tau)}{\pi t} dt \quad (2)$$

The phases $\varphi_j(t)$ for each parcel can be calculated directly from z(t):

$$\varphi(t) = \arctan\left(\frac{H[s(t)]}{s(t)}\right) \quad (3)$$

2.5. Kuramoto Order Parameter

The Kuramoto Order Parameter (KOP) measures the global level of synchronicity of multiple oscillators and is defined in equation below, where $\varphi_j(t)$ is the signal phase of an oscillator j at a given time. In our study, each brain parcel (AAL region) is treated as an independent oscillator.

$$KOP(t) = \frac{1}{N}\left|\sum_{\forall j=1}^{N} e^{i\varphi_j(t)}\right| \quad (4)$$

Once KOP was obtained for every time point, we obtained the mean KOP (synchrony aggregate over time, hereafter referred to as "*mean synchronisation*"), KOP standard deviation (hereafter referred to as "*metastability*") (Deco et al., 2017; Wildie and Shanahan, 2012). Mean KOP provides a broad measure of whole brain synchronicity, whereas metastability provides a measure of how synchronisation between different oscillators fluctuates over time, i.e., brain flexibility (Deco et al., 2017; Hellyer et al., 2015, 2014).

2.6. The Leading Eigenvector Analysis

KOP analyses can provide insight on global dynamic properties over all oscillators (brain parcels); but cannot inform which specific brain structures might be involved in those changes. To evaluate such modular (local) properties we applied the LEiDA approach – which allowed us to investigate phase coherence in different sets of parcels. To do so we first calculated the phase difference between a parcel i and a parcel j at every instant (TR), using the cosine distance:

$$\Delta\varphi_{ij}(t)=cos\left(\varphi_j(t)-\varphi_i(t)\right) \quad (5)$$

This results in a symmetric dynamic functional connectivity matrix for each fMRI volume. We then obtain a lower-dimensional representation with the LEiDA approach (Cabral et al., 2017; Gomes et al., 2020; Lord et al., 2019; Vohryzek et al., 2020), whereby the LEiDA vector corresponds to the first eigenvector of the decomposition of the matrix $\Delta\varphi_{ij}(t)$. This method has been previously shown to reveal information on the community structure of networks and graphs (Newman, 2006a, 2006b). Once the LEiDA vectors were obtained, we clustered them using K-Means (Cabral et al., 2017; Lord et al., 2019) with the optimal K (six) determined heuristically with the Calinski-Harabasz (Caliński and Harabasz, 1974) and Davies-Bouldin (Davies and Bouldin, 1979) methods (Supplementary Figure S3).

Each cluster represents a set of LEiDAs, and we refer to each of these as a *brain state*. The dynamics of such states can be studied with three main metrics: fractional occupancy – which refers to the total proportion of time spent in a given state or probability of that state; dwelling time – which consists of the average continuous time spent on each state; and Markovian probabilities of transitions between each state (Cabral et al., 2017; Lord et al., 2019). In addition, we also calculated values for mean synchronisation and metastability for each state by averaging those for the volumes belonging to each cluster.

2.7. Statistics

Firstly, we restricted our sample to the term-born individuals only (n = 324) and evaluated the effect of normative brain maturation and ex-utero experience (with PMA and PND at scan, respectively) in global and modular brain dynamics. Secondly, we evaluated the effects of

prematurity in brain dynamics by studying the entire sample of 390 individuals. Finally, we evaluated the association of global and modular dynamic features with later neurodevelopmental outcomes at 18 months corrected age (n = 305 – Bayley-III; n = 300 – Q-CHAT).

2.7.1. Global dynamics

We characterised the effect of age and postnatal experience (PMA and PND at scan) by fitting the linear model GLM1 (324 term-born babies): $y \sim \beta_0 + \beta_1 PMA + \beta_2 PND + \beta_3 Sex + \beta_4 [Motion\ outliers\ (FD)]$. To characterise the effect of preterm birth on brain dynamics, we fitted the linear model GLM2 (324 term-born and 66 preterm-born babies): $y \sim \beta_0 + \beta_1 Preterm\text{-}born + \beta_2 PMA + \beta_3 Sex + \beta_4 [Motion\ outliers\ (FD)]$. We assessed the association of brain global dynamics with cognitive and behavioural outcome measures, i.e., Bayley and Q-CHAT, at 18 months in a model given by GLM3 (257 term-born and 48 preterm-born babies for Bayley's scores; and 254 term-born and 46 preterm-born babies for Q-CHAT): $y \sim \beta_0 + \beta_1 GA + \beta_2 PMA + \beta_3 Sex + \beta_4 [Motion\ outliers\ (FD)] + \beta_5 [Corrected\ age\ at\ assessment] + \beta_6 [Assessed\ Component] + \beta_7 [Index\ of\ Multiple\ Deprivation]$ (with *Assessed Component* consisting of Bayley's cognitive, Bayley's language, Bayley's motor, or Q-CHAT total scores).

2.7.2. Modular dynamics: brain states

Firstly, we tested differences between the brain states defined in this study in terms of their mean synchronisation, metastability, fractional occupancy, and dwelling times per subject via a type III ANOVA with Satterthwaite's method (Giesbrecht and Burns, 1985; Hrong-Tai Fai and Cornelius, 1996; Kuznetsova et al., 2017) and the linear mixed effects model GLME1 (including 324 term-born): $y \sim \beta_0 + \beta_1 State + (1 \mid Subject\ ID)$ – with Subject ID accounting for the random effect. By fitting GLM1 (324 term-born babies): $y \sim \beta_0 + \beta_1 PMA + \beta_2 PND + \beta_3 Sex + \beta_4 [Motion\ outliers\ (FD)]$, we characterised the effect of age (PMA at scan) and postnatal experience (PND at scan) on fractional occupancy, dwelling times, mean synchronisation, and metastability for each of the six brain states.

Secondly, to characterise the effect of preterm birth on brain states and state-change probabilities, we fitted GLM2 (324 term-born and 66 preterm-born babies): $y \sim \beta_0 + \beta_1 Preterm\text{-}born + \beta_2 PMA + \beta_3 Sex + \beta_4 [Motion\ outliers\ (FD)]$ and GLM3 (324 term-born and 66 preterm-born babies): $y \sim \beta_0 + \beta_1 GA + \beta_2 PMA + \beta_3 Sex + \beta_4 [Motion\ outliers\ (FD)]$.

Thirdly, we assessed the association of brain dynamics with neurodevelopmental outcome measures (i.e., Bayley and Q-CHAT at 18 months) in a model given by GLM4 (257 term-born and 48 preterm-born babies for Bayley; and 254 term-born and 46 preterm-born babies for Q-CHAT): $y \sim \beta_0 + \beta_1 GA + \beta_2 PMA + \beta_3 Sex + \beta_4 [Motion\ outliers\ (FD)] + \beta_5 [Corrected\ age\ at\ assessment] + \beta_6 [Assessed\ component] + \beta_7 [Index\ of\ Multiple\ Deprivation]$ (with *Assessed Component* consisting of Bayley's cognitive, Bayley's language, Bayley's motor, or Q-CHAT total scores).

2.7.3. Statistical significance and repeated measures

We evaluated the statistical significance of each variable of interest with permutation tests with 10,000 repetitions for all GLMs. P-values are reported uncorrected, highlighting those surviving multiple comparison correction using the False Discovery Rate method with α at 5% (Benjamini and Hochberg, 1995).

2.7.4. Data and software availability

The fMRI datasets and clinical data analysed in this study are available as part of the dHCP's third data release, which can be obtained from https://data.developingconnectome.org. Pre-processed BOLD timeseries data used in this study are available in https://dx.doi.org/10.5281/zenodo.7053984. Dynamic properties of the BOLD signal fluctuations were then assessed with dynFC: CoDe-Neuro's Dynamic Functional Connectivity Tools (França and Batalle, 2022a), a set of scripts written in Python v3.7 (Van Rossum, 2020), and supporting libraries *Numpy* (Harris et al., 2020), *SciPy* (Virtanen et al., 2020), *Scikit-learn* (Pedregosa et al., 2011), *pickle*, *h5py*, *pandas* (McKinney, 2010; The pandas development team, 2020), *os*, *sys*, and *feather*.

Statistics and figures were produced in R programming language (R Core Team, 2021) and auxiliary packages *ggplot2* (Wickham, 2016, p. 2), *tidyr* (Wickham, 2021a), *dplyr* (Wickham et al., 2021), *cowplot* (Wilke, 2020a), *purrr* (Henry and Wickham, 2020), *RColorBrewer* (Neuwirth, 2014), *knitr* (Xie, 2021, 2015, 2014), *janitor* (Firke, 2021), *ggExtra* (Attali and Baker, 2019), *stringr* (Wickham, 2019), *rjson* (Couture-Beil, 2018), *broom* (Robinson et al., 2021), *Tidymodels* (Kuhn and Wickham, 2020), *shadowtext* (Yu, 2021a), *effsize* (Torchiano, 2020), modelr (Wickham, 2020), ggimage (Yu, 2021b), ggpubr (Kassambara, 2020), *patchwork* (Pedersen, 2020), *ggbeeswarm* (Clarke and Sherrill-Mix, 2017), *ggrepel* (Slowikowski, 2022), *ggtext* (Wilke, 2020b), *MetBrewer* (Mills, 2022), *lmerTest* (Kuznetsova et al., 2017), *forcats* (Wickham, 2021b), *stateR* (França and Batalle, 2022b), *p-testR* (França et al., 2022), *broom.mixed* (Bolker and Robinson, 2021), *lme4* (Bates et al., 2015, p. 4), and *DiagrammeR* (Iannone, 2020).

Brain volume images were produced with BrainNet Viewer (Xia et al., 2013) and Tools for NIfTI and ANALYZE images (Shen, 2014). All scripts used in this article's statistics and figures; and relevant instructions on how to run them, are available in https://github.com/CoDe-Neuro/neonatal_dfc.

3. Results

3.1. Global dynamics

We first assessed the association of global dynamic features with age at scan and postnatal experience (PMA and PND at scan, respectively) in only term-born individuals (Table 2). We did not observe any associations between PMA at scan and global dynamic features. Nevertheless, there was an association between PND at scan with metastability (t = -2.4; p = 0.017). In comparison to these term-born infants, preterm-born infants had lower mean synchrony (D = 0.567 – medium effect size; $p < 0.001$) and metastability (D = 0.454 – medium effect size; $p < 0.001$) (Figure 1AB, Table 2). Across the whole cohort, there was no significant association between metastability and any neurodevelopmental outcome, although mean synchronisation showed a weak but significant association with Q-CHAT scores (t = -2.57; p = 0.011), i.e., lower neonatal mean synchronisation was associated with higher Q-CHAT scores, indicative of more atypical social, sensory, and repetitive behaviours at 18 months of age (Figure 1C).

Table 2 Association of global dynamic features (synchrony and metastability) with PMA and PND at scan, and effect of preterm birth.

	Term (n = 324)				Term vs Preterm (n = 390)			
	PMA at scan		PND at scan		Term (n = 324)	Preterm (n = 66)	Cohen's D	p-value††
	t†	p-value†	t†	p-value†	[mean (S.D.)]			
Mean synchronisation	0.039	0.970	1.143	0.259	0.52 (0.08)	0.48 (0.08)	0.567	$p <$ 0.001*
Metastability	0.877	0.379	-2.403	0.017*	0.20 (0.02)	0.19 (0.02)	0.454	$p <$ 0.001*

*†GLM1 (including 324 term-born babies): $y \sim \beta_0 + \beta_1 PMA + \beta_2 PND + \beta_3 Sex + \beta_4 Motion$ outliers (FD). ††GLM2 (including 324 term-born and 66 preterm-born babies): $y \sim \beta_0 + \beta_1 Preterm\text{-}born + \beta_2 PMA + \beta_3 Sex + \beta_4 Motion$ outliers (FD). * p-values surviving multiple comparison correction (FDR).*

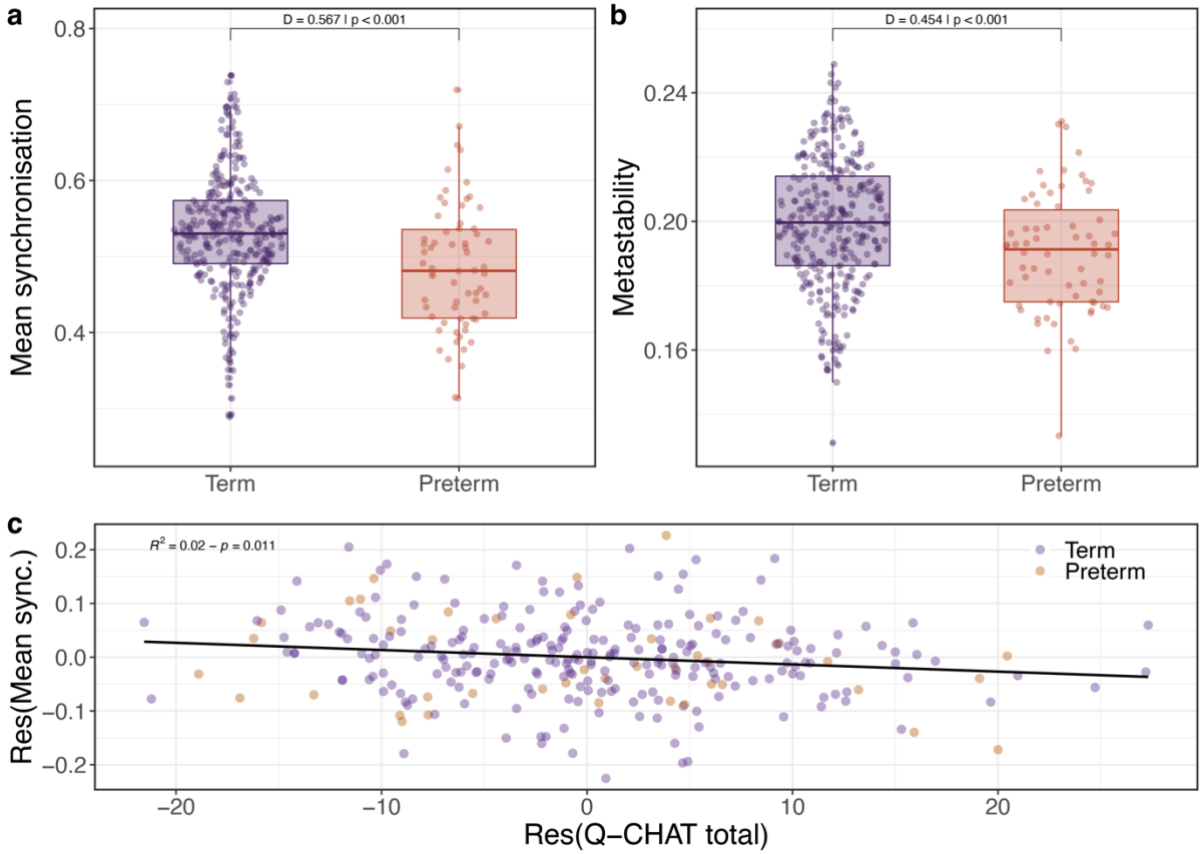

Figure 1 Effect of preterm-birth on mean synchronisation (**A**) and metastability (**B**); and correlation of mean synchronisation and Q-CHAT residuals (Res.) after correcting for PMA at scan, sex, motion outliers and preterm-birth (**C**).

3.2. Modular dynamics: brain states

We defined six different brain states, obtained heuristically from K-Means clustering, using the LEiDA approach (Figure 2). Three of the six states showed widespread phase concordance amongst the parcels, we refer to these as *whole-brain global synchronisation states*, namely *global state A*, *global state B* and *global state C*. Three states were more regionally constrained: one state showed synchronous phases in the *occipital* cortex; one state represented high synchrony for regions mainly in the *sensory-motor* cortex; and one state comprised high levels of synchronisation in the frontal cortex, angular gyrus, and posterior cingulate gyrus (for simplicity we refer to this as a '*frontoparietal state*').

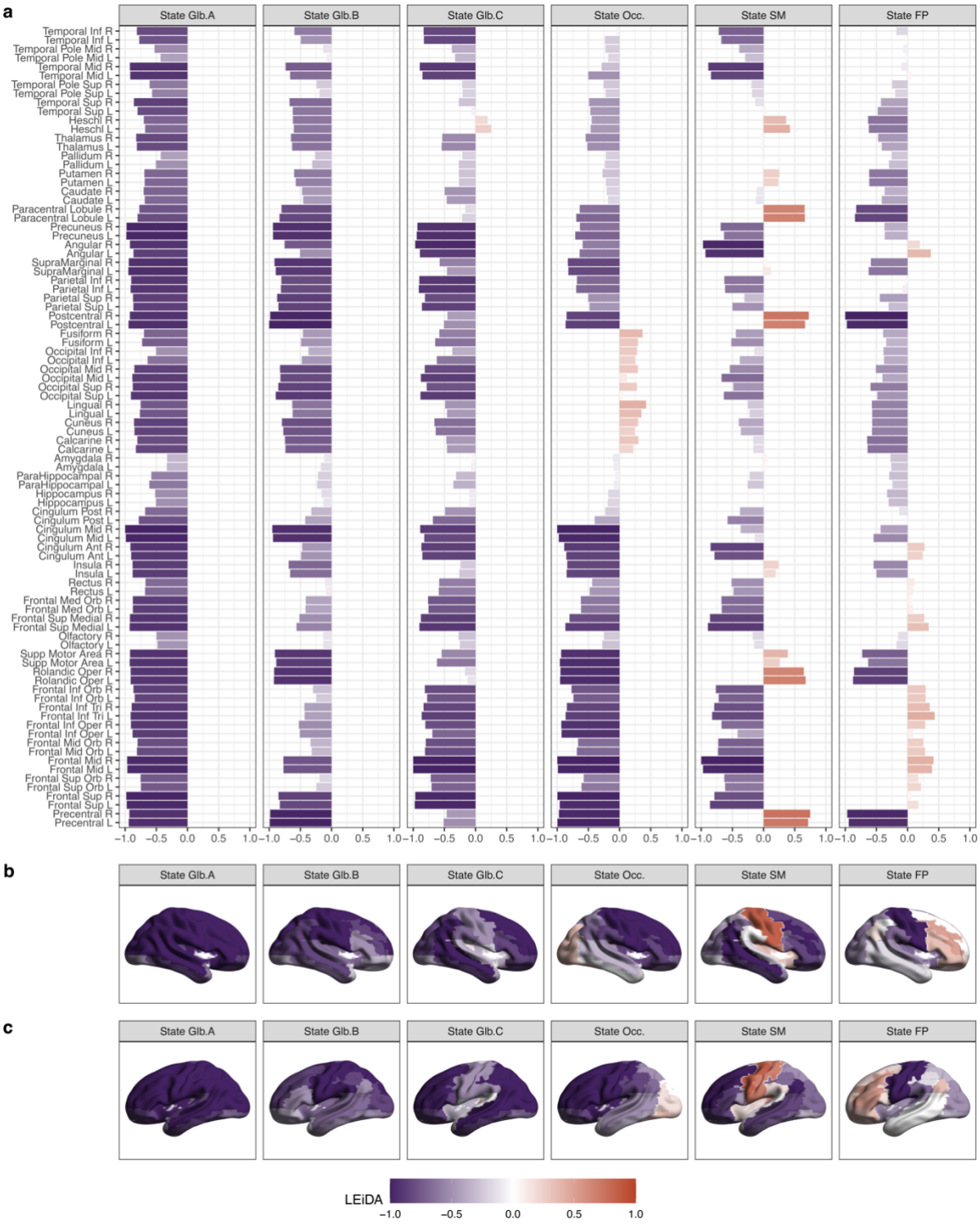

Figure 2 Brain states in neonates, ordered from left to right by level of global synchronicity. (**A**) LEiDA vectors for each of the six brain states previously obtained in this study. (**B**) Representation of LEiDA on brain surfaces (right side view). (**C**) Representation of LEiDA on brain surfaces (left side view).

3.2.1. Brain states in term-born children

3.2.1.1. Characteristic landscape of brain states

We compared the main dynamic features between the six identified states in term-born participants. There were significant differences between states in mean synchronisation, metastability, fractional occupancy, and dwelling times when tested using a type III ANOVA model with Satterthwaite's method: $F(5, 1615) = 13163$; $p < 0.001$ for mean synchronisation, $F(5, 1615) = 291$; $p < 0.001$ for mean metastability, $F(5, 1938) = 514$; $p < 0.001$ for mean fractional occupancy, and $F(5, 1938) = 734$; $p < 0.001$ for mean dwelling times. Between state effects showed that global state A had increased mean synchronisation, mean fractional occupancy, and mean dwelling times when compared with the other 5 states. Moreover, global states B and C also had a heightened mean synchronisation which was intermediate between the values recorded for global state A and the other states (see Supplementary Figure S4 for between-group effects statistics).

We characterised the normative brain state transition probabilities landscape in Figure 3A. Most occurrences are those of dwelling transitions, i.e., repeated continuous occurrences of the same state, with probabilities above 83% for all six states. Excluding those dwelling sequences, the 12 most frequent transitions displayed a complex profile, incorporating an indirect transition to and from the high whole-brain synchronisation global state A. These transitions occurred via the intermediate whole-brain synchronisation global states, B and C (Figure 3B).

3.2.1.2. Association of brain state features with age at scan

Higher PMA at scan was positively correlated with increased dwelling times (t =4.4; $p < 0.001$), increased fractional occupancy ($t = 5.3$, $p < 0.001$), and increased mean synchronisation ($t = 3.6$; $p < 0.001$) for global state C; and with increased fractional occupancy ($t = 2.8$, $p < 0.001$) and mean synchronisation in the sensory-motor state ($t = 3.1$; $p = 0.002$). PMA was negatively correlated with increased fractional occupancy in the global state B ($t = -2.8$; $p = 0.004$).

Postnatal age (PND at scan) was associated with shorter dwelling times in the global state B ($t = -2.8$; $p = 0.004$), occipital state ($t = -2.5$; $p = 0.013$), and sensory-motor state ($t = -2.8$; $p = 0.006$). Significant associations of brain state features with PMA and PND at scan are summarised in Figure 3C and Figure 3D; and compared in Figure 4G.

3.2.1.3 Association of brain state transitions with age at scan

Higher PMA at scan was positively associated with an increased likelihood of transitioning from global state A to C ($t = 3.2$; $p = 0.002$), from global state B to frontoparietal state ($t = 3.1$; $p = 0.002$), and to stay (dwell) in global state C ($t = 3.2$; $p = 0.001$). Older PMA was also associated with a lower likelihood of transitioning from global state C to occipital state ($t = -2.8$; $p = 0.006$); and lower probability of staying in global state B ($t = -2.9$; $p = 0.005$). Significant associations of state transition probabilities with PMA at scan are shown in Figure 3E.

Increased postnatal age (PND at scan) was associated with increased transitions from frontoparietal and occipital states into global state B [($t = 3.1$; $p = 0.002$) and ($t = 3.3$; $p = 0.001$), respectively]; increased transition from the occipital state into state C ($t = 3.1$; $p = 0.002$); a reduction of transition likelihood from state B into a frontoparietal state ($t = -3.0$; $p =$

0.003); and a reduction of probability to stay (dwell) in state C (t = -2.7; p = 0.007), occipital state (t = -3.4; p = 0.001), and sensory-motor state (t = -2.7; p = 0.007). Significant associations of state transition probabilities with PND at scan are shown in Figure 3F. For a comparison of the distinct effect of age (PMA at scan) and postnatal experience (PND at scan) in brain state transitions see Figure 4H. Age at scan and postnatal experience had distinct correlates: for example, transitions from intermediate whole-brain synchronisation state B to the occipital state increased with PMA at scan but decreased with PND at scan.

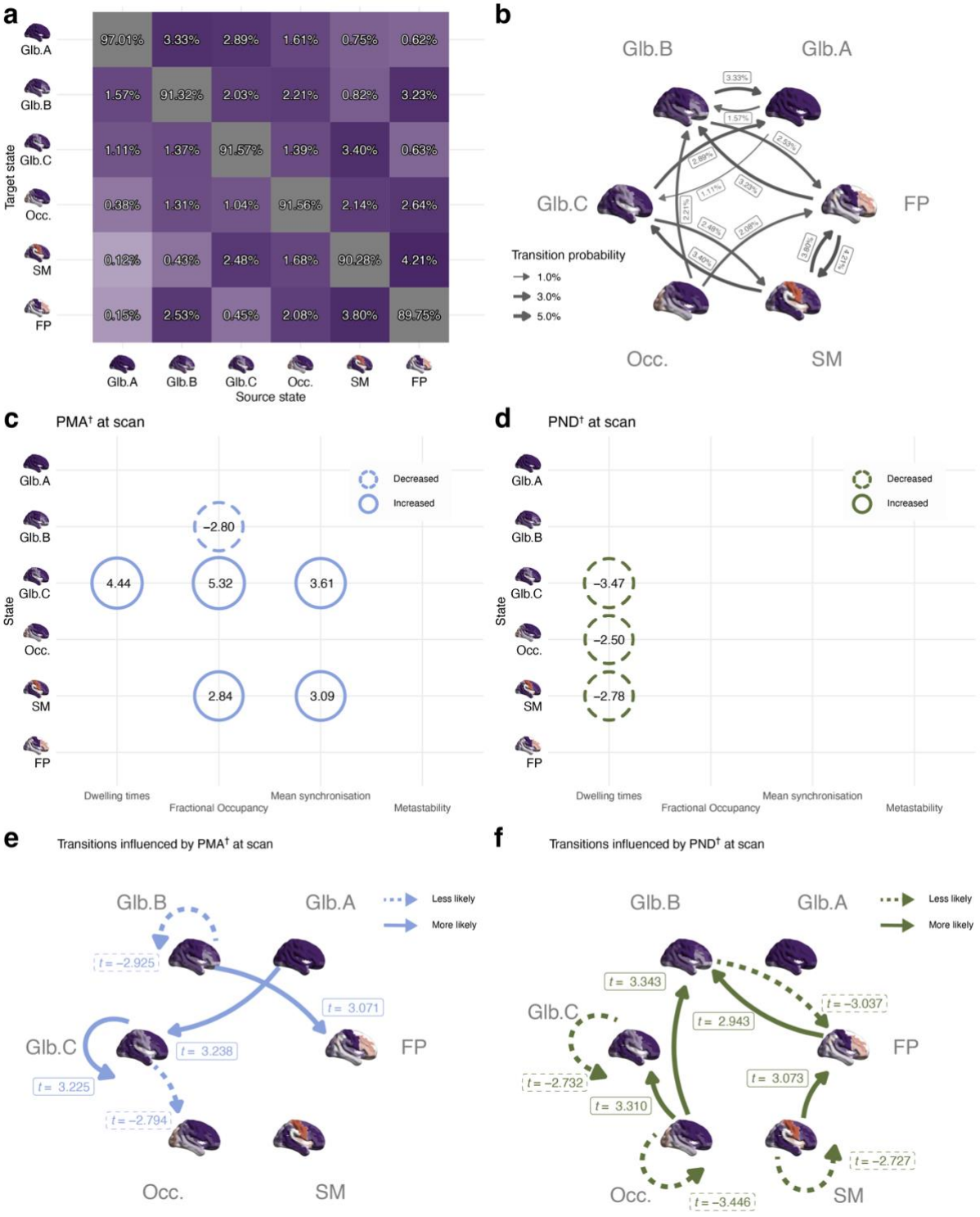

Figure 3 Brain dynamics in term-born children (n = 324). (**A**) All transitions including dwelling state transitions. (**B**) Main transitions (top 12) between states excluding dwelling transitions. (**C**) Summary of brain state features significantly associated with PMA at scan. (**D**) Summary of brain state features significantly associated with PND at scan. (**E**) Summary of significant correlations between state transitions probabilities and PMA at scan. (**F**) Summary of significant correlations between state transitions probabilities and PND at scan. †GLM1 (including 324 term-born babies): $y \sim \beta_0 + \beta_1\text{PMA} + \beta_2\text{PND} + \beta_3\text{Sex} + \beta_4\text{Motion outliers (FD)}$. Occ.: Occipital. SM: Sensory-motor. FP: Frontoparietal.

3.2.2. Effect of preterm birth on brain dynamics

3.2.2.1 Association of preterm birth with brain state features

Compared to term-born participants, preterm-born babies had shorter dwelling times for the global state A (t = -4.6; p < 0.001, Figure 4A); decreased fractional occupancy for the global state A (t = -4.1; p < 0.001); and increased fractional occupancy for global state B (t = 3.4; p = 0.001), occipital state (t = 2.2; p = 0.03), and frontoparietal state (t = 2.7; p = 0.009) (Figure 4B). Preterm birth was also associated with lower mean synchronisation of global state A (t = -5.1; p < 0.001), global state B (t = -3.4; p = 0.001), global state C (t = -2.8; p = 0.005), occipital state (t = -2.2; p = 0.031), and frontoparietal state (t = -2.6; p = 0.010)) (Figure 4C); and reduced metastability for the global state A (t = -2.5; p = 0.014) and frontoparietal state (t = -4.3; p < 0.001) (Figure 4D). Significant associations of brain state features with preterm birth are summarised in Figure 4E.

3.2.2.2 Association of preterm birth with brain state transition probability

Preterm birth was associated with an increased transition towards an occipital connectivity profile, i.e., an increased transition probability from global state A to C (t = 4.7; p = < 0.001) and from global state C to occipital (t = 3.1; p = 0.002); as well as a reduction in the probability staying (dwelling) in global state A (t = -4.4; p < 0.001); see Figure 4F. A similar profile of results was obtained when assessing how brain dynamic features changed with gestational age at birth which essentially captures preterm and term birth, see Supplementary Figure S5. Significant changes in transition probabilities associated with preterm-birth, and how they related to associations with PMA and PND at scan are summarised in Figure 4H.

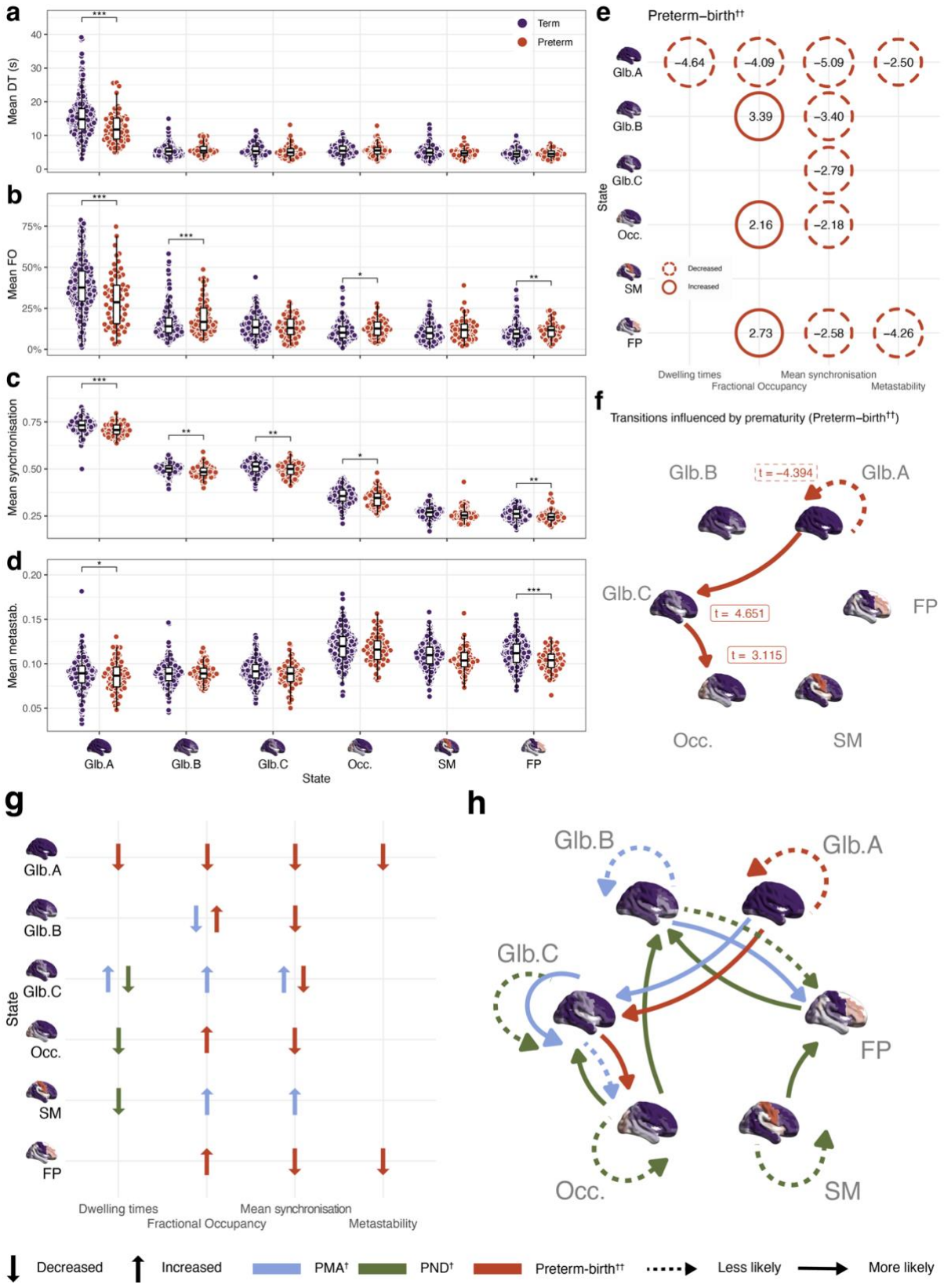

Figure 4 Effect of preterm birth in brain dynamics. (**A**) Mean dwelling times (DT). (**B**) Mean fractional occupancy (FO). (**C**) Mean synchronisation. (**D**) Metastability. (**E**) Summary of significant associations with preterm birth (**F**) Association of state transitions probabilities and preterm birth. (**G**) Summary of brain state features significantly associated with preterm birth, and comparison with those significantly associated with PMA and PND at scan. (**H**)

Summary of brain state transition probabilities associated with increased PMA, increased PND, and/or preterm-birth. †GLM1 (324 term-born babies): $y \sim \beta_0 + \beta_1 PMA + \beta_2 PND + \beta_3 Sex + \beta_4 Motion\ outliers\ (FD)$. ††GLM2 (324 term-born and 66 preterm-born babies): $y \sim \beta_0 + \beta_1 Preterm\text{-}born + \beta_2 PMA + \beta_3 Sex + \beta_4 Motion\ outliers\ (FD)$. * $p < 0.05$. ** $p < 0.01$. *** $p < 0.001$. Occ.: Occipital. SM: Sensory-motor. FP: Frontoparietal.

3.2.3. Associations with neurodevelopment

Higher mean synchronisation of the sensory-motor state in neonates was associated with poorer performance on both Bayley's cognitive and motor scores assessed later in childhood, at 18 months of age (t = -3.2, p = 0.002; and t = -3.4, p = 0.002 respectively; Figure 5A).

Higher Q-CHAT scores at 18 months of age were associated with higher fractional occupancy of sensory-motor state and reduced fractional occupancy of global state A (t = 2.5, p = 0.014; and t = -2.6, p = 0.010 respectively; Figure 5B).

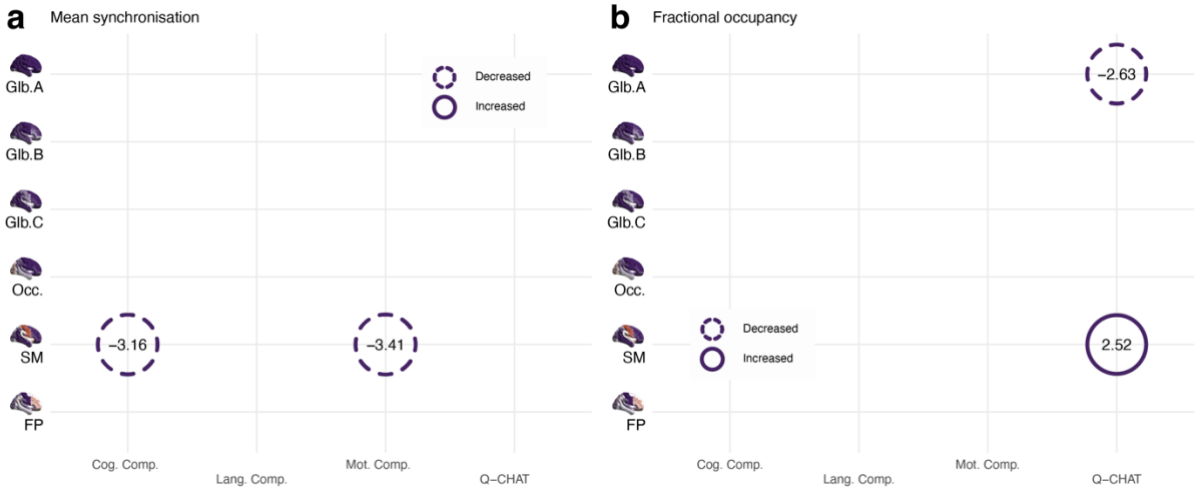

Figure 5 Summary of associations of brain state features with neurodevelopmental outcomes at 18 months corrected age. (**A**) Mean synchronisation and (**B**) Fractional occupancy of the six defined brain states during perinatal period. GLM3 (257 term-born and 48 preterm-born babies for Bayley; and 254 term-born and 46 preterm-born babies for Q-CHAT): $y \sim \beta_0 + \beta_1 GA + \beta_2 PMA + \beta_3 Sex + \beta_4 Motion\ outliers\ (FD) + \beta_5 Corrected\ age\ at\ assessment + \beta_6 Assessed\ component + \beta_7 Index\ of\ multiple\ deprivation$.

4. Discussion

In this study, we used global and modular fMRI signal analysis tools to investigate the characteristics of dynamic functional connectivity in a large sample of term and preterm born neonates. This is, to our knowledge, the first study to characterise these fundamental characteristics of brain dynamics this early in human development. We found that preterm birth

disrupted brain dynamics and that the profile of brain dynamics in early postnatal life is associated with a range of early childhood neurodevelopmental and behavioural outcomes at 18 months of age.

4.1. Global dynamics

We found that global dynamic features remained relatively stable through early development (PMA at scan) in a term-born population, although lower metastability was seen with more postnatal days at scan, suggesting that ex-utero life experience reduces brain dynamic flexibility after birth, and promotes more stable connectivity patterns. This is consistent with our observation that preterm born infants scanned at term equivalent age, and thus with greater exposure to postnatal life experience at the time of scan, had lower metastability than term born children. However, preterm babies also had lower mean synchronisation at term-equivalent age suggesting a unique pattern of alteration in brain dynamics associated with preterm birth which is independent of the extent of ex-utero life exposure (PND at scan). Lower metastability has been previously associated with impairments in cognitive flexibility of mature individuals after traumatic brain injury (Hellyer et al., 2015). However, the negative association between duration of postnatal life and metastability observed here is unlikely to relate to cognitive flexibility, but rather reflect a refinement of network dynamics driven by primary sensory stimulation associated with ex-utero life experience. Metastability seems to be additionally reduced by term equivalent age in preterm born babies, which may be consistent with theories suggesting perinatal stress atypically accelerates brain maturation, with potentially negative long-term impact (Tooley et al., 2021).

Our study extends prior work which has observed that, later in childhood, very preterm born infants have suboptimal neural synchrony and altered global dynamic connectivity patterns when scanned later in childhood (Padilla et al., 2020). Our metrics indicate that the impact of preterm birth on brain dynamics begins much earlier in life. Such differences in preterm-born babies may have their roots in alterations in the framework of structural and functional networks reported to accompany preterm birth. For example, previous studies have shown that preterm birth is associated with altered brain structure (Ment et al., 2009; Rogers et al., 2018), global functional architecture (Ball et al., 2016; Eyre et al., 2021), and structural network changes in the neonatal period (Batalle et al., 2017) which continue to be present at school-age (Fischi-Gomez et al., 2016) and into young adulthood (Karolis et al., 2016; Nosarti et al., 2014).

Global dynamic features were linked to later behaviour: lower mean synchronisation in the neonatal brain was associated with higher Q-CHAT scores at 18 months. Although high scores on the Q-CHAT indicate more autistic traits, in this study, the Q-CHAT captured a continuum of social, sensory, and repetitive behaviours across the normal distribution (Allison et al., 2008, 2021). Thus, while global metrics might usefully signpost the trajectory of foundational dynamic steps of human brain development, their association with Q-CHAT should not be over-interpreted as our study was not a study of ASD and we did not examine children at an age where neurodevelopmental diagnoses begin to be formalised.

4.2. Modular Brain state profile in term-born neonates

Summary metrics of global dynamics are likely themselves to be underpinned by much more complex activity. Therefore, we explored the emergence and behaviour of modular brain states in the early postnatal period. We characterised six transient states in the newborn brain at term equivalent age. Amongst the three states that showed widespread concordance (global states A-C), the first encompassed nearly all of the analysed cortical regions, the second showed a higher contribution of all sensory regions (auditory, sensory-motor, and visual) and the third state showed a higher contribution of visual and frontoparietal cortices. The other three states had a more restricted/regional span with distinct contributions from sensory-motor, visual and frontoparietal regions. The majority of these states thus encompassed primary sensory networks which are already known to mature earlier than higher order networks (Doria et al., 2010; Eyre et al., 2021; Smyser et al., 2010). This adds confidence to the results reported in earlier preliminary studies of dynamic FC in neonates around birth. For example, Ma et al., 2020, described dynamic functional connectivity with four brain states that encompassed default-mode, dorsal attention, auditory, sensory-motor, and visual networks in 37 term neonates (Ma et al., 2020). Here we establish a series of six brain states and describe associations with age at scan and postnatal days in a larger cohort with 324 term neonates.

We observed that in newborn infants, whole-brain synchrony state A had the highest mean synchronisation, as well as largest fractional occupancy and dwelling times; thus suggesting that newborn infants spend a large amount of their time in a state of global phase synchrony which is a similar to the previously described dominant pattern of whole-brain synchronisation seen with both fMRI (Ma et al., 2020; Wen et al., 2020) and EEG (Tokariev et al., 2019). Together with prior studies, our work supports the idea that large scale activity plays a crucial role in early brain development. Our results also align with the concept that this activity could support large scale cortical network formation and may foster the associated long-range connections, which are known to subsequently mature during the first postnatal year (Damaraju et al., 2014; Tau and Peterson, 2010).

4.3. Age-related changes in modular brain states

We observed a positive correlation of occupancy and mean synchronisation within the sensory-motor cortices with increasing PMA at scan. This supports existing evidence that this system is relatively mature, both in function and structure in comparison to other systems at birth. This may be the product of significant short-range functional reorganisation during the last foetal trimester (Cao et al., 2017; Dall'Orso et al., 2022) to support the functional specificity needed to respond to sensory information coming from feet, hands and mouth (Allievi et al., 2016; Dall'Orso et al., 2018).

We also found that increased PMA at scan, was associated with an increased probability of transitioning into frontoparietal synchronicity states comprising the anterior part of the Default Mode Network (DMN) (Buckner et al., 2008). This chimes with other evidence that, although this system is relatively immature at birth, it undergoes significant changes postnatally with increasing recruitment of frontoparietal areas into the network (Doria et al., 2010; Eyre et al.,

2021). Our work suggests that this system is recruited more and more with age in the postnatal period.

There was also a significant effect of PND at scan on an increasing probability of transition from occipital to whole-brain synchronisation states. This finding is in line with key stages of neurodevelopment. Specifically, changes in transitions from an occipital cortex profile may help the maturation of visuomotor abilities and sensory integration in early infancy in the environment outside the womb (Culham et al., 2006). Finally, we observed increased transitions from sensory-motor to frontoparietal structures with increasing duration of postnatal life, perhaps reflecting a move from a reliance on predominantly sensory-motor system output to behaviour informed by the higher order functions subserved by frontoparietal regions.

4.4. Effect of preterm birth on modular brain states

Preterm birth is associated with a higher likelihood of atypical neurodevelopment (Boardman and Counsell, 2020) including a greater rate of autism diagnosis (Agrawal et al., 2018; Joseph et al., 2017; Leviton et al., 2018; Limperopoulos et al., 2008; Raybaud et al., 2013; Schieve et al., 2016). Previous studies from our group have shown preterm born infants have alterations in their functional architecture (Ball et al., 2016; Doria et al., 2010; Eyre et al., 2021). Here, we extend this work to report that preterm birth also has an impact on dynamic functional connectivity, increasing fractional occupancy of occipital and frontal states and increased transitions from global to occipital state; and decreased dwelling for high whole-brain synchronisation state. Only one other study has investigated the effect of prematurity on dynamic functional connectivity (Ma et al., 2020). They reported significantly shorter mean dwelling times in a state with stronger connectivity between sensory-motor and auditory cortices and significantly higher mean dwelling times for a global state (Ma et al., 2020). Direct comparison with our findings is challenging however, given the higher resolution of our study in terms of a larger number of ROIs included in our study but also the power available from our larger sample. We observed multiple global states in neonates with diverse contributions from occipital and frontoparietal regions and a negative effect of prematurity on dwelling times in state A. In summary, preterm-birth shifts dynamic functional connectivity towards occipital and frontoparietal synchrony profiles and suppresses whole-brain synchronisation modes. Preterm-birth is known to impact on cognition throughout the lifespan (Brydges et al., 2018; Kroll et al., 2017). Our results raise the possibility, that alterations in brain functional connectivity that are present soon after birth have functional consequences.

4.5. Associations with neurodevelopment

Our work and others consistently recognises the neonatal period as a key time for sensory-motor cortical development (Allievi et al., 2016; Cao et al., 2017; Dall'Orso et al., 2018) and subsequent transition to higher order network connectivity (Doria et al., 2010; Eyre et al., 2021). We extended this observation here, to show that altered brain dynamics contributes to

both general developmental outcomes and more specific social, sensory, and repetitive behaviours at age 18 months. Lower levels of synchrony in the sensory-motor state around term were positively correlated with better cognitive and motor outcomes (Bayley-III) at 18 months. However, when there was lower fractional occupancy of the high whole-brain synchronisation state A and increased fractional occupancy of the sensory-motor state around birth, there were more atypical social, sensory, and repetitive traits present at 18 months, as captured by the Q-CHAT.

Thus, our work indicates that the link between brain dynamics and autistic traits is not only limited to state transitions in adulthood (Esfahlani et al., 2022; Watanabe and Rees, 2017) but may comprise alterations in state occupancy and overall synchronicity as well as transitions established during early development. One possible explanation for the association between the sensory-motor cortex dynamics and later social, sensory and repetitive traits, is that altered brain dynamics in the neonatal period may predispose individuals to exhibit unusual responses to sensory stimuli (Rogers and Ozonoff, 2005). The positive correlation of higher fractional occupancy of the sensory-motor state and a higher Q-CHAT score could also represent an overreliance on that particular network during the neonatal period – which may impact upon the development of higher order networks in the general population as a continuum.

We emphasize that we did not follow-up the children with higher Q-CHAT scores beyond 18 months, thus our work did not evaluate predictors of a confirmed diagnosis of ASD. Longitudinal studies are clearly needed, but our work adds to the evidence for persistent dysmaturation of sensory systems to autistic features across the lifespan. Sensory differences are among the first features to signal a diagnosis of ASD (Kolesnik et al., 2019; Tomchek and Dunn, 2007) and persist, remaining core to the diagnosis (American Psychiatric Association, 2013). For example, we have reported that neonates with an increased familial likelihood of ASD had higher regional homogeneity in the sensory-motor cortex (Ciarrusta et al., 2020), which fits with the higher fractional occupancy we record in this region. Studies of diagnosed individuals have reported atypical activation of the motor cortex (Martineau et al., 2010), which likely affects the translation of visual input into motor understanding, with a potential impact on social interaction. These functional brain differences in sensory systems are thought to arise from alterations in excitation-inhibition pathways, especially GABA neurotransmission. Evidence includes a tight relationship between sensory processing and differences in sensory cortex GABA levels (Puts et al., 2017) and we have reported direct experimental proof in adults, that visual processing differences in ASD are GABA-dependent (Huang et al., 2022).

4.6. Strengths and limitations

We studied state-of-the-art infant fMRI acquired with a dedicated neonatal multiband EPI pipeline which features high temporal resolution (TR = 392 ms) but acknowledge this has relatively low signal-to-noise ratio in the deep grey matter (thalamus, basal ganglia, brainstem) structures (Fitzgibbon et al., 2020).

We chose a LEiDA processing pipeline, as it provides time-resolved metrics of brain states and has been successfully applied to study brain dynamics in adults (Cabral et al., 2017; Figueroa et al., 2019; Gomes et al., 2020; Lord et al., 2019; Vohryzek et al., 2020). Although a majority

of prior studies of dynamic brain functional connectivity have adopted sliding window approaches, it necessitates the choice of arbitrary parameters in the analysis, such as window and step sizes. There is little consensus on these parameters as the use of small windows can magnify spurious variations and large windows can soften sharper changes in brain dynamics (Leonardi and Van De Ville, 2015; Preti et al., 2017; Savva et al., 2019). Thus, the choice of a time-resolved approach like LEiDA is a strength in our methodology.

However, our analysis treated brain state occurrence in an independent fashion, i.e., without memory. Future studies could benefit from developing a metric that considers how brain states are impacted by previously occurring states. Our results are also potentially limited by the use of the AAL atlas which has been validated for neonatal use (Shi et al., 2011) to define our regions of interest. Such structurally defined atlases could potentially poorly correlate with functional boundaries in the brain, particularly during the neonatal period (Sala-Llonch et al., 2019; Smith et al., 2013). A possible solution for future work could be the adaptation and use of multi-modal generated surface atlases (Glasser et al., 2016) for neonatal fMRI studies.

In our analysis, we didn't consider the effect of socio-demographic factors and social deprivation beyond using the Index of Multiple Deprivation scores as a covariate. However, multiples studies have shown that family psychosocial and socio-demographic factors have a significant impact on brain development in childhood; with factors such as maternal stress, depression, low education, maternal immigration status, maternal age greater than 35 years, paternal age over 38 years and low household income all being linked to poorer developmental outcomes (Deave et al., 2008; Dollaghan et al., 1999; Gale-Grant et al., 2020; Glover and O'Connor, 2002; Leonard et al., 2011; Rice et al., 2010; To et al., 2004). Thus, further studies could benefit from evaluating links between these wider socio-demographic markers and brain dynamics in early childhood (Gale-Grant et al., 2022).

5. Conclusions

In this study we evaluated global functional brain dynamics and transient brain states in the newborn brain. Our approach allowed us to define a set of six fundamental transient brain states, which are comprised by structures previously shown to be established in earlier phases of brain development. We have highlighted the impact brain maturation has on brain dynamics, as well as atypical patterns associated with preterm birth. Brain state dynamics at birth appear to be functionally relevant as they are correlated with a range of neurodevelopmental outcomes in early childhood. This encourages further work to understand their prognostic value and regulation to guide support and intervention where appropriate.

Funding

This work was supported by the European Research Council under the European Union's Seventh Framework Programme (FP7/20072013)/ERC grant agreement no. 319456 (dHCP project) and a Wellcome Trust Seed Award in Science [217316/Z/19/Z]. The authors

acknowledge infrastructure support from the National Institute for Health Research (NIHR) Mental Health Biomedical Research Centre (BRC) at South London, Maudsley NHS Foundation Trust and Institute of Psychiatry, Psychology and Neuroscience, King's College London and the NIHR-BRC at Guys and St Thomas' Hospitals NHS Foundation Trust (GSTFT). The authors also acknowledge support in part from the Wellcome Engineering and Physical Sciences Research Council (EPSRC) Centre for Medical Engineering at Kings College London [WT 203148/Z/16/Z], MRC strategic grant [MR/K006355/1], Medical Research Council Centre grant [MR/N026063/1], the Department of Health through an NIHR Comprehensive Biomedical Research Centre Award (to Guy's and St. Thomas' National Health Service (NHS) Foundation Trust in partnership with King's College London and King's College Hospital NHS Foundation Trust), the Sackler Institute for Translational Neurodevelopment at King's College London and the European Autism Interventions (EU-AIMS) trial and the EU AIMS-2-TRIALS, a European Innovative Medicines Initiative Joint Undertaking under Grant Agreements No. 115300 and 777394, the resources of which are composed of financial contributions from the European Union's Seventh Framework Programme (Grant FP7/2007–2013). SFM is supported by a grant from the UK Medical Research Council [MR/N013700/1]. OGG is supported by a grant from the UK Medical Research Council [MR/P502108/1]. JOM, TA, GM and ADE received support from the Medical Research Council Centre for Neurodevelopmental Disorders, King's College London [MR/N026063/1]. LCG is supported by a Beatriz Galindo Fellowship from MCIU/UPM-Spain [BGP18/00178] and line Support for R&D Projects for Beatriz Galindo researchers from CAM-Spain. JJT was supported by grants from the Finnish Medical Foundation, Sigrid Juselius Foundation, Signe and Ane Gyllenberg Foundation and Emil Aaltonen Foundation. JOM is supported by a Sir Henry Dale Fellowship jointly funded by the Wellcome Trust and the Royal Society [206675/Z/17/Z]. TA is supported by an MRC Clinician Scientist Fellowship [MR/P008712/1] and Transition Support Award [MR/V036874/1]. The authors acknowledge use of the research computing facility at King's College London, Rosalind (https://rosalind.kcl.ac.uk), which is delivered in partnership with the National Institute for Health Research (NIHR) Biomedical Research Centres at South London & Maudsley and Guy's & St. Thomas' NHS Foundation Trusts, and part-funded by capital equipment grants from the Maudsley Charity (award 980) and Guy's & St. Thomas' Charity (TR130505). The views expressed are those of the authors and not necessarily those of the NHS, the National Institute for Health Research, or the Department of Health. The funders had no role in the design and conduct of the study; collection, management, analysis, and interpretation of the data; preparation, review, or approval of the manuscript; and decision to submit the manuscript for publication.

Competing interests

The authors report no competing interests.

Supplementary

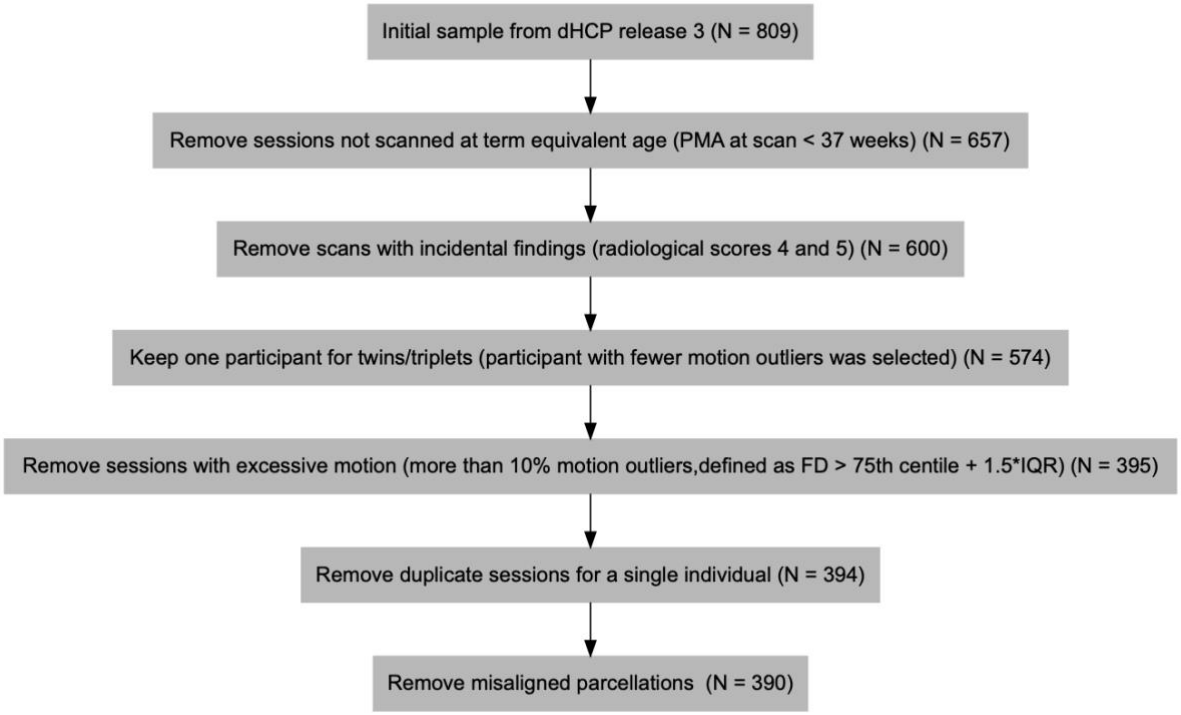

Supplementary Figure S1 Exclusion criteria flowchart.

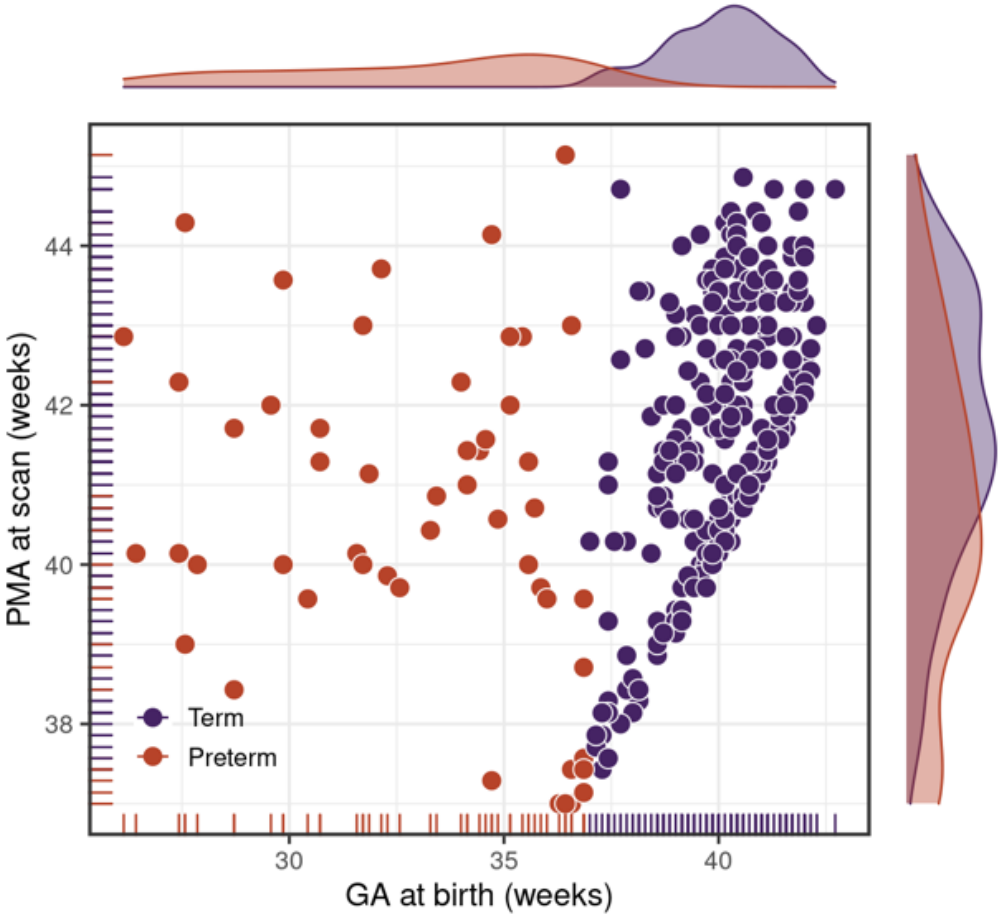

Supplementary Figure S2 Distribution of gestational age (GA) at birth and postmentrual age (PMA) at scan for the individuals selected for this study.

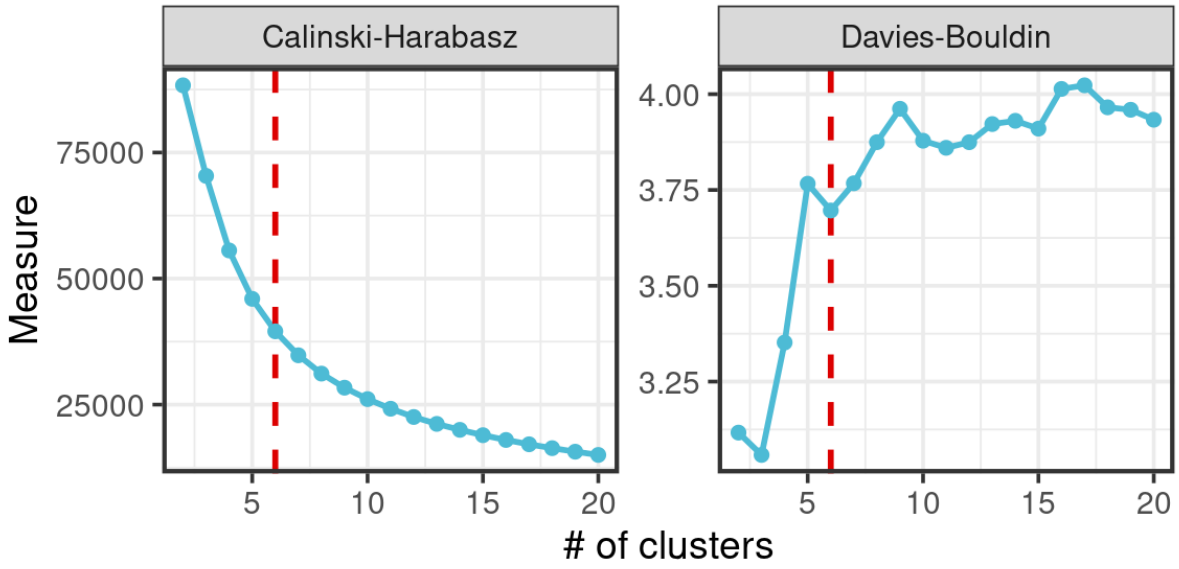

Supplementary Figure S3 Ideal number of clusters according to Calinski-Harabasz and Davies-Bouldin methods.

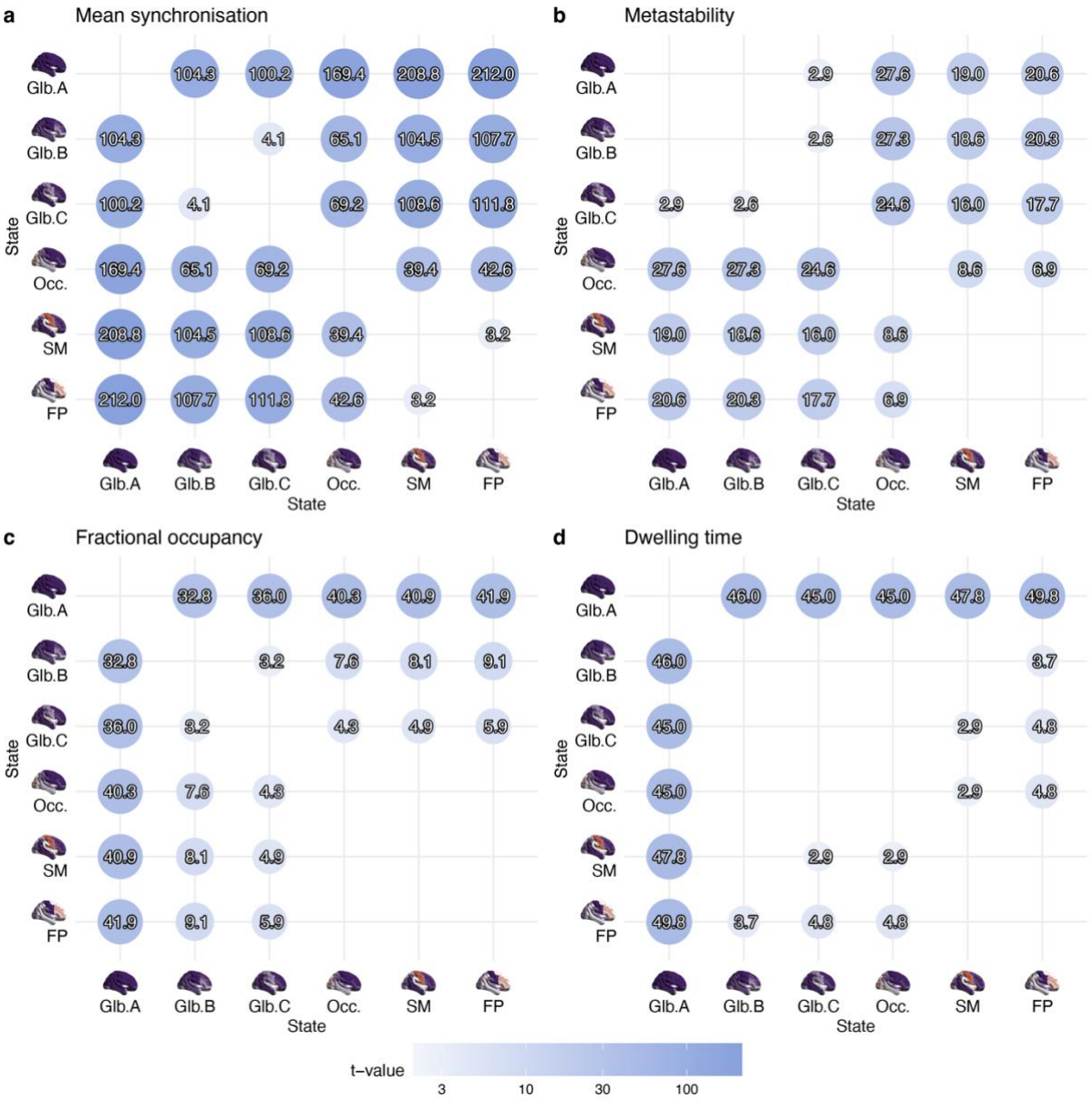

Supplementary Figure S4 ANOVA post-hoc tests for a) Mean synchronisation, b) Metastability, c) fractional occupancy, and d) dwelling times.

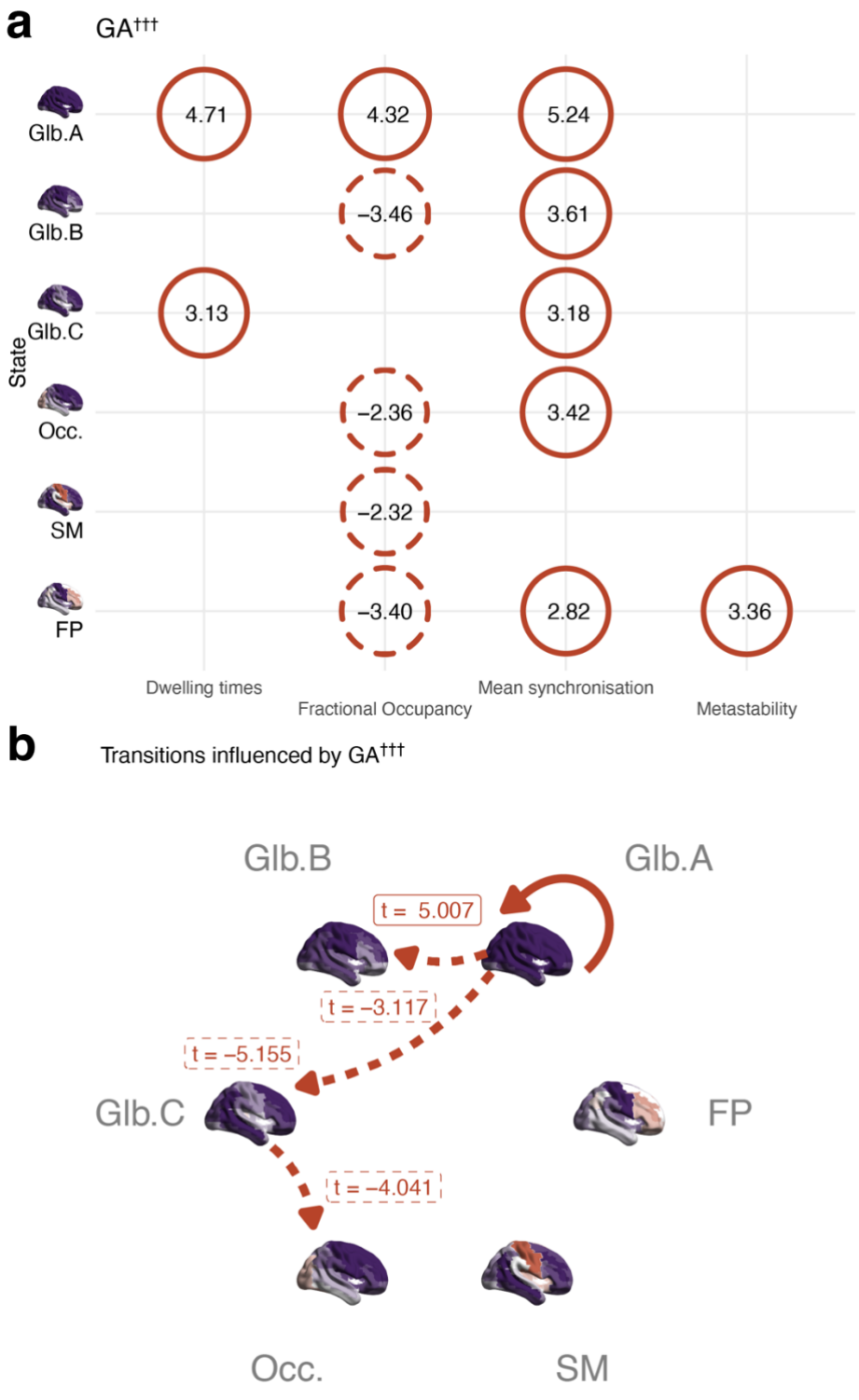

Supplementary Figure S5 Modular analysis of neonatal brain dynamics. (**A**) Summary of associations between each of the four metrics (dwelling times, fractional occupancy, mean synchronisation, metastability) and GA at birth. (**B**) Association of state transitions probabilities and GA at birth. †††GLM3 (including 324 term-born and 66 preterm-born babies): $y \sim \beta_0 + \beta_1 \text{GA} + \beta_2 \text{PMA} + \beta_3 \text{Sex} + \beta_4 \text{Motion outliers (FD)}$. * $p < 0.05$. ** $p < 0.01$. *** $p < 0.001$. Occ.: Occipital. SM: Sensory-motor. FP: Frontoparietal.

References

Abel, G.A., Barclay, M.E., Payne, R.A., 2016. Adjusted indices of multiple deprivation to enable comparisons within and between constituent countries of the UK including an illustration using mortality rates. BMJ Open 6, e012750. https://doi.org/10.1136/bmjopen-2016-012750

Agrawal, S., Rao, S.C., Bulsara, M.K., Patole, S.K., 2018. Prevalence of Autism Spectrum Disorder in Preterm Infants: A Meta-analysis. Pediatrics 142, e20180134. https://doi.org/10.1542/peds.2018-0134

Allen, E.A., Damaraju, E., Plis, S.M., Erhardt, E.B., Eichele, T., Calhoun, V.D., 2014. Tracking Whole-Brain Connectivity Dynamics in the Resting State. Cerebral Cortex 24, 663–676. https://doi.org/10.1093/cercor/bhs352

Allievi, A.G., Arichi, T., Tusor, N., Kimpton, J., Arulkumaran, S., Counsell, S.J., Edwards, A.D., Burdet, E., 2016. Maturation of Sensori-Motor Functional Responses in the Preterm Brain. Cerebral Cortex 26, 402–413. https://doi.org/10.1093/cercor/bhv203

Allison, C., Baron-Cohen, S., Wheelwright, S., Charman, T., Richler, J., Pasco, G., Brayne, C., 2008. The Q-CHAT (Quantitative CHecklist for Autism in Toddlers): A Normally Distributed Quantitative Measure of Autistic Traits at 18–24 Months of Age: Preliminary Report. J Autism Dev Disord 38, 1414–1425. https://doi.org/10.1007/s10803-007-0509-7

Allison, C., Matthews, F.E., Ruta, L., Pasco, G., Soufer, R., Brayne, C., Charman, T., Baron-Cohen, S., 2021. Quantitative Checklist for Autism in Toddlers (Q-CHAT). A population screening study with follow-up: the case for multiple time-point screening for autism. bmjpo 5, e000700. https://doi.org/10.1136/bmjpo-2020-000700

American Psychiatric Association, 2013. Diagnostic and Statistical Manual of Mental Disorders, Fifth Edition. ed. American Psychiatric Association. https://doi.org/10.1176/appi.books.9780890425596

Andersson, J.L.R., Graham, M.S., Drobnjak, I., Zhang, H., Filippini, N., Bastiani, M., 2017. Towards a comprehensive framework for movement and distortion correction of diffusion MR images: Within volume movement. NeuroImage 152, 450–466. https://doi.org/10.1016/j.neuroimage.2017.02.085

Andersson, J.L.R., Skare, S., Ashburner, J., 2003. How to correct susceptibility distortions in spin-echo echo-planar images: application to diffusion tensor imaging. NeuroImage 20, 870–888. https://doi.org/10.1016/S1053-8119(03)00336-7

Andersson, J.L.R., Sotiropoulos, S.N., 2016. An integrated approach to correction for off-resonance effects and subject movement in diffusion MR imaging. NeuroImage 125, 1063–1078. https://doi.org/10.1016/j.neuroimage.2015.10.019

Attali, D., Baker, C., 2019. ggExtra: Add Marginal Histograms to "ggplot2", and More "ggplot2" Enhancements.

Avants, B.B., Tustison, N.J., Song, G., Cook, P.A., Klein, A., Gee, J.C., 2011. A reproducible evaluation of ANTs similarity metric performance in brain image registration. NeuroImage 54, 2033–2044. https://doi.org/10.1016/j.neuroimage.2010.09.025

Ball, G., Aljabar, P., Arichi, T., Tusor, N., Cox, D., Merchant, N., Nongena, P., Hajnal, J.V., Edwards, A.D., Counsell, S.J., 2016. Machine-learning to characterise neonatal functional connectivity in the preterm brain. NeuroImage 124, 267–275. https://doi.org/10.1016/j.neuroimage.2015.08.055

Batalle, D., Hughes, E.J., Zhang, H., Tournier, J.-D., Tusor, N., Aljabar, P., Wali, L., Alexander, D.C., Hajnal, J.V., Nosarti, C., Edwards, A.D., Counsell, S.J., 2017. Early development of structural networks and the impact of prematurity on brain connectivity. NeuroImage 149, 379–392. https://doi.org/10.1016/j.neuroimage.2017.01.065

Bates, D., Mächler, M., Bolker, B., Walker, S., 2015. Fitting Linear Mixed-Effects Models Using lme4. Journal of Statistical Software 67, 1–48. https://doi.org/10.18637/jss.v067.i01

Bayley, N., 2006. Bayley scales of infant and toddler development–Third Edition: Technical manual.

Benjamini, Y., Hochberg, Y., 1995. Controlling the False Discovery Rate: A Practical and Powerful Approach to Multiple Testing. Journal of the Royal Statistical Society: Series B (Methodological) 57, 289–300. https://doi.org/10.1111/j.2517-6161.1995.tb02031.x

Boardman, J.P., Counsell, S.J., 2020. Invited Review: Factors associated with atypical brain development in preterm infants: insights from magnetic resonance imaging. Neuropathol Appl Neurobiol 46, 413–421. https://doi.org/10.1111/nan.12589

Boashash, B., 1992. Estimating and interpreting the instantaneous frequency of a signal. I. Fundamentals. Proc. IEEE 80, 520–538. https://doi.org/10.1109/5.135376

Bolker, B., Robinson, D., 2021. broom.mixed: Tidying Methods for Mixed Models.

Brydges, C.R., Landes, J.K., Reid, C.L., Campbell, C., French, N., Anderson, M., 2018. Cognitive outcomes in children and adolescents born very preterm: a meta-analysis. Dev Med Child Neurol 60, 452–468. https://doi.org/10.1111/dmcn.13685

Buckner, R.L., Andrews-Hanna, J.R., Schacter, D.L., 2008. The Brain's Default Network Anatomy, Function, and Relevance to Disease. Annals of the New York Academy of Sciences 1124, 1–38. https://doi.org/10.1196/annals.1440.011

Cabral, J., Vidaurre, D., Marques, P., Magalhães, R., Silva Moreira, P., Miguel Soares, J., Deco, G., Sousa, N., Kringelbach, M.L., 2017. Cognitive performance in healthy older adults relates to spontaneous switching between states of functional connectivity during rest. Scientific Reports 7, 5135. https://doi.org/10.1038/s41598-017-05425-7

Calhoun, V.D., Miller, R., Pearlson, G., Adalı, T., 2014. The Chronnectome: Time-Varying Connectivity Networks as the Next Frontier in fMRI Data Discovery. Neuron 84, 262–274. https://doi.org/10.1016/j.neuron.2014.10.015

Caliński, T., Harabasz, J., 1974. A dendrite method for cluster analysis. null 3, 1–27. https://doi.org/10.1080/03610927408827101

Cao, M., He, Y., Dai, Z., Liao, X., Jeon, T., Ouyang, M., Chalak, L., Bi, Y., Rollins, N., Dong, Q., Huang, H., 2017. Early Development of Functional Network Segregation Revealed by Connectomic Analysis of the Preterm Human Brain. Cerebral cortex 27, 1949–1963. https://doi.org/10.1093/cercor/bhw038

Chyl, K., Fraga-González, G., Brem, S., Jednoróg, K., 2021. Brain dynamics of (a)typical reading development—a review of longitudinal studies. npj Sci. Learn. 6, 4. https://doi.org/10.1038/s41539-020-00081-5

Ciarrusta, J., Dimitrova, R., Batalle, D., O'Muircheartaigh, J., Cordero-Grande, L., Price, A., Hughes, E., Kangas, J., Perry, E., Javed, A., Demilew, J., Hajnal, J., Edwards, A.D., Murphy, D., Arichi, T., McAlonan, G., 2020. Emerging functional connectivity differences in newborn infants vulnerable to autism spectrum disorders. Transl Psychiatry 10, 131. https://doi.org/10.1038/s41398-020-0805-y

Clarke, E., Sherrill-Mix, S., 2017. ggbeeswarm: Categorical Scatter (Violin Point) Plots.

Couture-Beil, A., 2018. rjson: JSON for R.

Culham, J.C., Cavina-Pratesi, C., Singhal, A., 2006. The role of parietal cortex in visuomotor control: What have we learned from neuroimaging? Neuropsychologia 44, 2668–2684. https://doi.org/10.1016/j.neuropsychologia.2005.11.003

Dall'Orso, S., Arichi, T., Fitzgibbon, S.P., Edwards, A.D., Burdet, E., Muceli, S., 2022. Development of functional organization within the sensorimotor network across the perinatal period. Human Brain Mapping 43, 2249–2261. https://doi.org/10.1002/hbm.25785

Dall'Orso, S., Steinweg, J., Allievi, A.G., Edwards, A.D., Burdet, E., Arichi, T., 2018. Somatotopic Mapping of the Developing Sensorimotor Cortex in the Preterm Human Brain. Cerebral Cortex 28, 2507–2515. https://doi.org/10.1093/cercor/bhy050

Damaraju, E., Caprihan, A., Lowe, J.R., Allen, E.A., Calhoun, V.D., Phillips, J.P., 2014. Functional connectivity in the developing brain: A longitudinal study from 4 to 9months of age. NeuroImage 84, 169–180. https://doi.org/10.1016/j.neuroimage.2013.08.038

Davies, D.L., Bouldin, D.W., 1979. A Cluster Separation Measure. IEEE Trans. Pattern Anal. Mach. Intell. PAMI-1, 224–227. https://doi.org/10.1109/TPAMI.1979.4766909

de Lacy, N., Calhoun, V.D., 2019. Dynamic connectivity and the effects of maturation in youth with attention deficit hyperactivity disorder. Network Neuroscience 3, 195–216. https://doi.org/10.1162/netn_a_00063

de Lacy, N., Doherty, D., King, B.H., Rachakonda, S., Calhoun, V.D., 2017. Disruption to control network function correlates with altered dynamic connectivity in the wider autism spectrum. NeuroImage: Clinical 15, 513–524. https://doi.org/10.1016/j.nicl.2017.05.024

Deave, T., Heron, J., Evans, J., Emond, A., 2008. The impact of maternal depression in pregnancy on early child development. BJOG: An International Journal of Obstetrics & Gynaecology 115, 1043–1051. https://doi.org/10.1111/j.1471-0528.2008.01752.x

Deco, G., Kringelbach, M.L., Jirsa, V.K., Ritter, P., 2017. The dynamics of resting fluctuations in the brain: metastability and its dynamical cortical core. Sci Rep 7, 3095. https://doi.org/10.1038/s41598-017-03073-5

Díez-Cirarda, M., Strafella, A.P., Kim, J., Peña, J., Ojeda, N., Cabrera-Zubizarreta, A., Ibarretxe-Bilbao, N., 2018. Dynamic functional connectivity in Parkinson's disease patients with mild cognitive impairment and normal cognition. NeuroImage: Clinical 17, 847–855. https://doi.org/10.1016/j.nicl.2017.12.013

Dollaghan, C.A., Campbell, T.F., Paradise, J.L., Feldman, H.M., Janosky, J.E., Pitcairn, D.N., Kurs-Lasky, M., 1999. Maternal Education and Measures of Early Speech and Language. J Speech Lang Hear Res 42, 1432–1443. https://doi.org/10.1044/jslhr.4206.1432

Doria, V., Beckmann, C.F., Arichi, T., Merchant, N., Groppo, M., Turkheimer, F.E., Counsell, S.J., Murgasova, M., Aljabar, P., Nunes, R.G., Larkman, D.J., Rees, G., Edwards, A.D., 2010. Emergence of resting state networks in the preterm human brain. Proceedings of the National Academy of Sciences 107, 20015–20020. https://doi.org/10.1073/pnas.1007921107

Edwards, A.D., Rueckert, D., Smith, S.M., Abo Seada, S., Alansary, A., Almalbis, J., Allsop, J., Andersson, J., Arichi, T., Arulkumaran, S., Bastiani, M., Batalle, D., Baxter, L., Bozek, J., Braithwaite, E., Brandon, J., Carney, O., Chew, A., Christiaens, D., Chung, R., Colford, K., Cordero-Grande, L., Counsell, S.J., Cullen, H., Cupitt, J., Curtis, C., Davidson, A., Deprez, M., Dillon, L., Dimitrakopoulou, K., Dimitrova, R., Duff, E., Falconer, S., Farahibozorg, S.-R., Fitzgibbon, S.P., Gao, J., Gaspar, A., Harper, N., Harrison, S.J., Hughes, E.J., Hutter, J., Jenkinson, M., Jbabdi, S., Jones, E., Karolis, V., Kyriakopoulou, V., Lenz, G., Makropoulos, A., Malik, S., Mason, L., Mortari, F., Nosarti, C., Nunes, R.G., O'Keeffe, C., O'Muircheartaigh, J., Patel, H., Passerat-Palmbach, J., Pietsch, M., Price, A.N., Robinson, E.C., Rutherford, M.A., Schuh, A., Sotiropoulos, S., Steinweg, J., Teixeira, R.P.A.G., Tenev, T., Tournier, J.-D., Tusor, N., Uus, A., Vecchiato, K., Williams, L.Z.J., Wright, R., Wurie, J., Hajnal, J.V., 2022. The Developing Human Connectome Project Neonatal Data Release. Front. Neurosci. 16, 886772. https://doi.org/10.3389/fnins.2022.886772

Engels, G., Vlaar, A., McCoy, B., Scherder, E., Douw, L., 2018. Dynamic Functional Connectivity and Symptoms of Parkinson's Disease: A Resting-State fMRI Study. Frontiers in Aging Neuroscience 10, 388. https://doi.org/10.3389/fnagi.2018.00388

Erb, J., Henry, M.J., Eisner, F., Obleser, J., 2013. The Brain Dynamics of Rapid Perceptual Adaptation to Adverse Listening Conditions. Journal of Neuroscience 33, 10688–10697. https://doi.org/10.1523/JNEUROSCI.4596-12.2013

Esfahlani, F.Z., Byrge, L., Tanner, J., Sporns, O., Kennedy, D.P., Betzel, R.F., 2022. Edge-centric analysis of time-varying functional brain networks with applications in autism spectrum disorder. NeuroImage 263, 119591. https://doi.org/10.1016/j.neuroimage.2022.119591

Eyre, M., Fitzgibbon, S.P., Ciarrusta, J., Cordero-Grande, L., Price, A.N., Poppe, T., Schuh, A., Hughes, E., O'Keeffe, C., Brandon, J., Cromb, D., Vecchiato, K., Andersson, J., Duff, E.P., Counsell, S.J., Smith, S.M., Rueckert, D., Hajnal, J.V., Arichi, T., O'Muircheartaigh, J., Batalle, D., Edwards, A.D., 2021. The Developing Human Connectome Project: typical and disrupted perinatal functional connectivity. Brain 144, 2199–2213. https://doi.org/10.1093/brain/awab118

Figueroa, C.A., Cabral, J., Mocking, R.J.T., Rapuano, K.M., Hartevelt, T.J., Deco, G., Expert, P., Schene, A.H., Kringelbach, M.L., Ruhé, H.G., 2019. Altered ability to access a clinically relevant control network in patients remitted from major depressive disorder. Human Brain Mapping 40, 2771–2786. https://doi.org/10.1002/hbm.24559

Firke, S., 2021. janitor: Simple Tools for Examining and Cleaning Dirty Data.

Fischi-Gomez, E., Muñoz-Moreno, E., Vasung, L., Griffa, A., Borradori-Tolsa, C., Monnier, M., Lazeyras, F., Thiran, J.-P., Hüppi, P.S., 2016. Brain network characterization of high-risk

preterm-born school-age children. NeuroImage: Clinical 11, 195–209. https://doi.org/10.1016/j.nicl.2016.02.001

Fitzgibbon, S.P., Harrison, S.J., Jenkinson, M., Baxter, L., Robinson, E.C., Bastiani, M., Bozek, J., Karolis, V., Cordero Grande, L., Price, A.N., Hughes, E., Makropoulos, A., Passerat-Palmbach, J., Schuh, A., Gao, J., Farahibozorg, S.-R., O'Muircheartaigh, J., Ciarrusta, J., O'Keeffe, C., Brandon, J., Arichi, T., Rueckert, D., Hajnal, J.V., Edwards, A.D., Smith, S.M., Duff, E., Andersson, J., 2020. The developing Human Connectome Project (dHCP) automated resting-state functional processing framework for newborn infants. NeuroImage 223, 117303. https://doi.org/10.1016/j.neuroimage.2020.117303

França, L.G.S., Batalle, D., 2022a. dynFC: CoDe-Neuro's Dynamic Functional Connectivity Tools. https://doi.org/10.5281/ZENODO.6615603

França, L.G.S., Batalle, D., 2022b. stateR. https://doi.org/10.5281/ZENODO.7053548

França, L.G.S., Ge, Y., Batalle, D., 2022. p-testR. https://doi.org/10.5281/ZENODO.7051925

Fransson, P., Skiöld, B., Engström, M., Hallberg, B., Mosskin, M., Åden, U., Lagercrantz, H., Blennow, M., 2009. Spontaneous Brain Activity in the Newborn Brain During Natural Sleep—An fMRI Study in Infants Born at Full Term. Pediatr Res 66, 301–305. https://doi.org/10.1203/PDR.0b013e3181b1bd84

Fransson, P., Skiöld, B., Horsch, S., Nordell, A., Blennow, M., Lagercrantz, H., Åden, U., 2007. Resting-state networks in the infant brain. Proc. Natl. Acad. Sci. U.S.A. 104, 15531–15536. https://doi.org/10.1073/pnas.0704380104

Gale-Grant, O., Chew, A., Falconer, S., Franca, L.G.S., Fenn-Moltu, S., Hadaya, L., Harper, N., Ciarrusta, J., Charman, T., Murphy, D., Arichi, T., McAlonan, G., Nosarti, C., Edwards, D., Batalle, D., 2022. Clinical, socio-demographic, and parental correlates of early autism traits. bioRxiv 2022.09.26.508121. https://doi.org/10.1101/2022.09.26.508121

Gale-Grant, O., Christiaens, D., Cordero-Grande, L., Chew, A., Falconer, S., Makropoulos, A., Harper, N., Price, A.N., Hutter, J., Hughes, E., Victor, S., Counsell, S.J., Rueckert, D., Hajnal, J.V., Edwards, A.D., O'Muircheartaigh, J., Batalle, D., 2020. Parental age effects on neonatal white matter development. NeuroImage: Clinical 27, 102283. https://doi.org/10.1016/j.nicl.2020.102283

Gao, W., Alcauter, S., Elton, A., Hernandez-Castillo, C.R., Smith, J.K., Ramirez, J., Lin, W., 2015a. Functional Network Development During the First Year: Relative Sequence and Socioeconomic Correlations. Cereb. Cortex 25, 2919–2928. https://doi.org/10.1093/cercor/bhu088

Gao, W., Alcauter, S., Smith, J.K., Gilmore, J.H., Lin, W., 2015b. Development of human brain cortical network architecture during infancy. Brain Struct Funct 220, 1173–1186. https://doi.org/10.1007/s00429-014-0710-3

Giesbrecht, F.G., Burns, J.C., 1985. Two-Stage Analysis Based on a Mixed Model: Large-Sample Asymptotic Theory and Small-Sample Simulation Results. Biometrics 41, 477. https://doi.org/10.2307/2530872

Glasser, M.F., Coalson, T.S., Robinson, E.C., Hacker, C.D., Harwell, J., Yacoub, E., Ugurbil, K., Andersson, J., Beckmann, C.F., Jenkinson, M., Smith, S.M., Van Essen, D.C., 2016. A multi-modal parcellation of human cerebral cortex. Nature 536, 171–178. https://doi.org/10.1038/nature18933

Glerean, E., Salmi, J., Lahnakoski, J.M., Jääskeläinen, I.P., Sams, M., 2012. Functional Magnetic Resonance Imaging Phase Synchronization as a Measure of Dynamic Functional Connectivity. Brain Connectivity 2, 91–101. https://doi.org/10.1089/brain.2011.0068

Glover, V., O'Connor, T.G., 2002. Effects of antenatal stress and anxiety: Implications for development and psychiatry. Br J Psychiatry 180, 389–391. https://doi.org/10.1192/bjp.180.5.389

Gomes, M.T., Fernandes, H.M., Cabral, J., 2020. Deep brain stimulation modulates the dynamics of resting-state networks in patients with Parkinson's Disease (preprint). Neuroscience. https://doi.org/10.1101/2020.11.04.368274

Gonzalez-Castillo, J., Bandettini, P.A., 2018. Task-based dynamic functional connectivity: Recent findings and open questions. NeuroImage 180, 526–533. https://doi.org/10.1016/j.neuroimage.2017.08.006

Griffanti, L., Salimi-Khorshidi, G., Beckmann, C.F., Auerbach, E.J., Douaud, G., Sexton, C.E., Zsoldos, E., Ebmeier, K.P., Filippini, N., Mackay, C.E., Moeller, S., Xu, J., Yacoub, E., Baselli, G., Ugurbil, K., Miller, K.L., Smith, S.M., 2014. ICA-based artefact removal and accelerated fMRI acquisition for improved resting state network imaging. NeuroImage 95, 232–247. https://doi.org/10.1016/j.neuroimage.2014.03.034

Harris, C.R., Millman, K.J., Walt, S.J. van der, Gommers, R., Virtanen, P., Cournapeau, D., Wieser, E., Taylor, J., Berg, S., Smith, N.J., Kern, R., Picus, M., Hoyer, S., Kerkwijk, M.H. van, Brett, M., Haldane, A., Río, J.F. del, Wiebe, M., Peterson, P., Gérard-Marchant, P., Sheppard, K., Reddy, T., Weckesser, W., Abbasi, H., Gohlke, C., Oliphant, T.E., 2020. Array programming with NumPy. Nature 585, 357–362. https://doi.org/10.1038/s41586-020-2649-2

Hellyer, P.J., Scott, G., Shanahan, M., Sharp, D.J., Leech, R., 2015. Cognitive Flexibility through Metastable Neural Dynamics Is Disrupted by Damage to the Structural Connectome. Journal of Neuroscience 35, 9050–9063. https://doi.org/10.1523/JNEUROSCI.4648-14.2015

Hellyer, P.J., Shanahan, M., Scott, G., Wise, R.J.S., Sharp, D.J., Leech, R., 2014. The Control of Global Brain Dynamics: Opposing Actions of Frontoparietal Control and Default Mode Networks on Attention. Journal of Neuroscience 34, 451–461. https://doi.org/10.1523/JNEUROSCI.1853-13.2014

Henry, L., Wickham, H., 2020. purrr: Functional Programming Tools.

Hrong-Tai Fai, Alex., Cornelius, P.L., 1996. Approximate F-tests of multiple degree of freedom hypotheses in generalized least squares analyses of unbalanced split-plot experiments. Journal of Statistical Computation and Simulation 54, 363–378. https://doi.org/10.1080/00949659608811740

Hughes, E.J., Winchman, T., Padormo, F., Teixeira, R., Wurie, J., Sharma, M., Fox, M., Hutter, J., Cordero-Grande, L., Price, A.N., Allsop, J., Bueno-Conde, J., Tusor, N., Arichi, T., Edwards, A.D., Rutherford, M.A., Counsell, S.J., Hajnal, J.V., 2017. A dedicated neonatal brain imaging system. Magnetic Resonance in Medicine 78, 794–804. https://doi.org/10.1002/mrm.26462

Hutchison, R.M., Womelsdorf, T., Allen, E.A., Bandettini, P.A., Calhoun, V.D., Corbetta, M., Della Penna, S., Duyn, J.H., Glover, G.H., Gonzalez-Castillo, J., Handwerker, D.A., Keilholz, S., Kiviniemi, V., Leopold, D.A., de Pasquale, F., Sporns, O., Walter, M., Chang, C., 2013. Dynamic functional connectivity: Promise, issues, and interpretations. NeuroImage 80, 360–378. https://doi.org/10.1016/j.neuroimage.2013.05.079

Iannone, R., 2020. DiagrammeR: Graph/Network Visualization.

Joseph, R.M., O'Shea, T.M., Allred, E.N., Heeren, T., Hirtz, D., Paneth, N., Leviton, A., Kuban, K.C.K., 2017. Prevalence and associated features of autism spectrum disorder in extremely low gestational age newborns at age 10 years: Prevalence of ASD among ELGANs. Autism Research 10, 224–232. https://doi.org/10.1002/aur.1644

Karolis, V.R., Froudist-Walsh, S., Brittain, P.J., Kroll, J., Ball, G., Edwards, A.D., Dell'Acqua, F., Williams, S.C., Murray, R.M., Nosarti, C., 2016. Reinforcement of the Brain's Rich-Club Architecture Following Early Neurodevelopmental Disruption Caused by Very Preterm Birth. Cereb. Cortex 26, 1322–1335. https://doi.org/10.1093/cercor/bhv305

Kassambara, A., 2020. ggpubr: "ggplot2" Based Publication Ready Plots.

Kolesnik, A., Begum Ali, J., Gliga, T., Guiraud, J., Charman, T., Johnson, M.H., Jones, E.J.H., The BASIS Team, 2019. Increased cortical reactivity to repeated tones at 8 months in infants with later ASD. Transl Psychiatry 9, 46. https://doi.org/10.1038/s41398-019-0393-x

Kroll, J., Karolis, V., Brittain, P.J., Tseng, C.-E.J., Froudist-Walsh, S., Murray, R.M., Nosarti, C., 2017. Real-Life Impact of Executive Function Impairments in Adults Who Were Born Very Preterm. J Int Neuropsychol Soc 23, 381–389. https://doi.org/10.1017/S1355617717000169

Kuhn, M., Wickham, H., 2020. Tidymodels: a collection of packages for modeling and machine learning using tidyverse principles.

Kuznetsova, A., Brockhoff, P.B., Christensen, R.H.B., 2017. **lmerTest** Package: Tests in Linear Mixed Effects Models. J. Stat. Soft. 82. https://doi.org/10.18637/jss.v082.i13

Leonard, H., Glasson, E., Nassar, N., Whitehouse, A., Bebbington, A., Bourke, J., Jacoby, P., Dixon, G., Malacova, E., Bower, C., Stanley, F., 2011. Autism and Intellectual Disability Are

Differentially Related to Sociodemographic Background at Birth. PLoS ONE 6, e17875. https://doi.org/10.1371/journal.pone.0017875

Leonardi, N., Van De Ville, D., 2015. On spurious and real fluctuations of dynamic functional connectivity during rest. NeuroImage 104, 430–436. https://doi.org/10.1016/j.neuroimage.2014.09.007

Leviton, A., Joseph, R.M., Allred, E.N., Fichorova, R.N., O'Shea, T.M., Kuban, K.K.C., Dammann, O., 2018. The risk of neurodevelopmental disorders at age 10 years associated with blood concentrations of interleukins 4 and 10 during the first postnatal month of children born extremely preterm. Cytokine 110, 181–188. https://doi.org/10.1016/j.cyto.2018.05.004

Limperopoulos, C., Bassan, H., Sullivan, N.R., Soul, J.S., Robertson, R.L., Moore, M., Ringer, S.A., Volpe, J.J., du Plessis, A.J., 2008. Positive Screening for Autism in Ex-preterm Infants: Prevalence and Risk Factors. Pediatrics 121, 758–765. https://doi.org/10.1542/peds.2007-2158

Lord, L.-D., Expert, P., Atasoy, S., Roseman, L., Rapuano, K., Lambiotte, R., Nutt, D.J., Deco, G., Carhart-Harris, R.L., Kringelbach, M.L., Cabral, J., 2019. Dynamical exploration of the repertoire of brain networks at rest is modulated by psilocybin. NeuroImage 199, 127–142. https://doi.org/10.1016/j.neuroimage.2019.05.060

Lurie, D.J., Kessler, D., Bassett, D.S., Betzel, R.F., Breakspear, M., Kheilholz, S., Kucyi, A., Liégeois, R., Lindquist, M.A., McIntosh, A.R., Poldrack, R.A., Shine, J.M., Thompson, W.H., Bielczyk, N.Z., Douw, L., Kraft, D., Miller, R.L., Muthuraman, M., Pasquini, L., Razi, A., Vidaurre, D., Xie, H., Calhoun, V.D., 2020. Questions and controversies in the study of time-varying functional connectivity in resting fMRI. Network Neuroscience 4, 30–69. https://doi.org/10.1162/netn_a_00116

Ma, X., Wu, X., Shi, Y., 2020. Changes of Dynamic Functional Connectivity Associated With Maturity in Late Preterm Infants. Front. Pediatr. 8, 412. https://doi.org/10.3389/fped.2020.00412

Makropoulos, A., Gousias, I.S., Ledig, C., Aljabar, P., Serag, A., Hajnal, J.V., Edwards, A.D., Counsell, S.J., Rueckert, D., 2014. Automatic Whole Brain MRI Segmentation of the Developing Neonatal Brain. IEEE Trans. Med. Imaging 33, 1818–1831. https://doi.org/10.1109/TMI.2014.2322280

Martineau, J., Andersson, F., Barthélémy, C., Cottier, J.-P., Destrieux, C., 2010. Atypical activation of the mirror neuron system during perception of hand motion in autism. Brain Research 1320, 168–175. https://doi.org/10.1016/j.brainres.2010.01.035

McKinney, W., 2010. Data Structures for Statistical Computing in Python, in: Walt, S. van der, Millman, J. (Eds.), Proceedings of the 9th Python in Science Conference. pp. 56–61. https://doi.org/10.25080/Majora-92bf1922-00a

Ment, L.R., Hirtz, D., Hüppi, P.S., 2009. Imaging biomarkers of outcome in the developing preterm brain. The Lancet Neurology 8, 1042–1055. https://doi.org/10.1016/S1474-4422(09)70257-1

Mills, B.R., 2022. MetBrewer: Color Palettes Inspired by Works at the Metropolitan Museum of Art.

Neuwirth, E., 2014. RColorBrewer: ColorBrewer Palettes.

Newman, M.E.J., 2006a. Modularity and community structure in networks. Proceedings of the National Academy of Sciences 103, 8577–8582. https://doi.org/10.1073/pnas.0601602103

Newman, M.E.J., 2006b. Finding community structure in networks using the eigenvectors of matrices. Physical Review E 74, 036104. https://doi.org/10.1103/PhysRevE.74.036104

Nosarti, C., Nam, K.W., Walshe, M., Murray, R.M., Cuddy, M., Rifkin, L., Allin, M.P.G., 2014. Preterm birth and structural brain alterations in early adulthood. NeuroImage: Clinical 6, 180–191. https://doi.org/10.1016/j.nicl.2014.08.005

Padilla, N., Saenger, V.M., van Hartevelt, T.J., Fernandes, H.M., Lennartsson, F., Andersson, J.L.R., Kringelbach, M., Deco, G., Åden, U., 2020. Breakdown of Whole-brain Dynamics in Preterm-born Children. Cerebral Cortex 30, 1159–1170. https://doi.org/10.1093/cercor/bhz156

Pedersen, T.L., 2020. patchwork: The Composer of Plots.

Pedregosa, F., Varoquaux, G., Gramfort, A., Michel, V., Thirion, B., Grisel, O., Blondel, M., Prettenhofer, P., Weiss, R., Dubourg, V., Vanderplas, J., Passos, A., Cournapeau, D., Brucher,

M., Perrot, M., Duchesnay, E., 2011. Scikit-learn: Machine Learning in Python. Journal of Machine Learning Research 12, 2825–2830.

Ponce-Alvarez, A., He, B.J., Hagmann, P., Deco, G., 2015. Task-Driven Activity Reduces the Cortical Activity Space of the Brain: Experiment and Whole-Brain Modeling. PLoS Comput Biol 11, e1004445. https://doi.org/10.1371/journal.pcbi.1004445

Power, J.D., Barnes, K.A., Snyder, A.Z., Schlaggar, B.L., Petersen, S.E., 2012. Spurious but systematic correlations in functional connectivity MRI networks arise from subject motion. NeuroImage 59, 2142–2154. https://doi.org/10.1016/j.neuroimage.2011.10.018

Power, J.D., Mitra, A., Laumann, T.O., Snyder, A.Z., Schlaggar, B.L., Petersen, S.E., 2014. Methods to detect, characterize, and remove motion artifact in resting state fMRI. NeuroImage 84, 320–341. https://doi.org/10.1016/j.neuroimage.2013.08.048

Preti, M.G., Bolton, T.A., Van De Ville, D., 2017. The dynamic functional connectome: State-of-the-art and perspectives. NeuroImage 160, 41–54. https://doi.org/10.1016/j.neuroimage.2016.12.061

Puts, N.A.J., Wodka, E.L., Harris, A.D., Crocetti, D., Tommerdahl, M., Mostofsky, S.H., Edden, R.A.E., 2017. Reduced GABA and altered somatosensory function in children with autism spectrum disorder: Abnormal GABA and touch in ASD. Autism Research 10, 608–619. https://doi.org/10.1002/aur.1691

R Core Team, 2021. R: A Language and Environment for Statistical Computing. R Foundation for Statistical Computing, Vienna, Austria.

Raybaud, C., Ahmad, T., Rastegar, N., Shroff, M., Al Nassar, M., 2013. The premature brain: Developmental and lesional anatomy. Neuroradiology 55, 23–40. https://doi.org/10.1007/s00234-013-1231-0

Rice, F., Harold, G.T., Boivin, J., van den Bree, M., Hay, D.F., Thapar, A., 2010. The links between prenatal stress and offspring development and psychopathology: disentangling environmental and inherited influences. Psychol. Med. 40, 335–345. https://doi.org/10.1017/S0033291709005911

Robinson, D., Hayes, A., Couch, S., 2021. broom: Convert Statistical Objects into Tidy Tibbles.

Rogers, C.E., Lean, R.E., Wheelock, M.D., Smyser, C.D., 2018. Aberrant structural and functional connectivity and neurodevelopmental impairment in preterm children. J Neurodevelop Disord 10, 38. https://doi.org/10.1186/s11689-018-9253-x

Rogers, S.J., Ozonoff, S., 2005. Annotation: What do we know about sensory dysfunction in autism? A critical review of the empirical evidence. J Child Psychol & Psychiat 46, 1255–1268. https://doi.org/10.1111/j.1469-7610.2005.01431.x

Sakoğlu, Ü., Pearlson, G.D., Kiehl, K.A., Wang, Y.M., Michael, A.M., Calhoun, V.D., 2010. A method for evaluating dynamic functional network connectivity and task-modulation: Application to schizophrenia. Magnetic Resonance Materials in Physics, Biology and Medicine 23, 351–366. https://doi.org/10.1007/s10334-010-0197-8

Sala-Llonch, R., Smith, S.M., Woolrich, M., Duff, E.P., 2019. Spatial parcellations, spectral filtering, and connectivity measures in fMRI: Optimizing for discrimination. Hum Brain Mapp 40, 407–419. https://doi.org/10.1002/hbm.24381

Salimi-Khorshidi, G., Douaud, G., Beckmann, C.F., Glasser, M.F., Griffanti, L., Smith, S.M., 2014. Automatic denoising of functional MRI data: Combining independent component analysis and hierarchical fusion of classifiers. NeuroImage 90, 449–468. https://doi.org/10.1016/j.neuroimage.2013.11.046

Savva, A.D., Mitsis, G.D., Matsopoulos, G.K., 2019. Assessment of dynamic functional connectivity in resting-state fMRI using the sliding window technique. Brain and Behavior 9, e01255. https://doi.org/10.1002/brb3.1255

Schaefer, A., Margulies, D.S., Lohmann, G., Gorgolewski, K.J., Smallwood, J., Kiebel, S.J., Villringer, A., 2014. Dynamic network participation of functional connectivity hubs assessed by resting-state fMRI. Frontiers in Human Neuroscience 8, 195. https://doi.org/10.3389/fnhum.2014.00195

Schieve, L.A., Tian, L.H., Rankin, K., Kogan, M.D., Yeargin-Allsopp, M., Visser, S., Rosenberg, D., 2016. Population impact of preterm birth and low birth weight on developmental disabilities

in US children. Annals of Epidemiology 26, 267–274. https://doi.org/10.1016/j.annepidem.2016.02.012

Schuh, A., Makropoulos, A., Robinson, E.C., Cordero-Grande, L., Hughes, E., Hutter, J., Price, A.N., Murgasova, M., Teixeira, R.P.A.G., Tusor, N., Steinweg, J.K., Victor, S., Rutherford, M.A., Hajnal, J.V., Edwards, A.D., Rueckert, D., 2018. Unbiased construction of a temporally consistent morphological atlas of neonatal brain development (preprint). Neuroscience. https://doi.org/10.1101/251512

Shen, J., 2014. Tools for NIfTI and ANALYZE image.

Shi, F., Yap, P.T., Wu, G., Jia, H., Gilmore, J.H., Lin, W., Shen, D., 2011. Infant brain atlases from neonates to 1- and 2-year-olds. PLoS ONE 6. https://doi.org/10.1371/journal.pone.0018746

Slowikowski, K., 2022. ggrepel: Automatically Position Non-Overlapping Text Labels with "ggplot2."

Smith, S.M., Vidaurre, D., Beckmann, C.F., Glasser, M.F., Jenkinson, M., Miller, K.L., Nichols, T.E., Robinson, E.C., Salimi-Khorshidi, G., Woolrich, M.W., Barch, D.M., Uğurbil, K., Van Essen, D.C., 2013. Functional connectomics from resting-state fMRI. Trends in Cognitive Sciences 17, 666–682. https://doi.org/10.1016/j.tics.2013.09.016

Smyser, C.D., Inder, T.E., Shimony, J.S., Hill, J.E., Degnan, A.J., Snyder, A.Z., Neil, J.J., 2010. Longitudinal Analysis of Neural Network Development in Preterm Infants. Cerebral Cortex 20, 2852–2862. https://doi.org/10.1093/cercor/bhq035

Smyser, C.D., Snyder, A.Z., Shimony, J.S., Mitra, A., Inder, T.E., Neil, J.J., 2016. Resting-State Network Complexity and Magnitude Are Reduced in Prematurely Born Infants. Cereb. Cortex 26, 322–333. https://doi.org/10.1093/cercor/bhu251

Tagliazucchi, E., Laufs, H., 2014. Decoding Wakefulness Levels from Typical fMRI Resting-State Data Reveals Reliable Drifts between Wakefulness and Sleep. Neuron 82, 695–708. https://doi.org/10.1016/j.neuron.2014.03.020

Tau, G.Z., Peterson, B.S., 2010. Normal Development of Brain Circuits. Neuropsychopharmacology 35, 147–168. https://doi.org/10.1038/npp.2009.115

The pandas development team, 2020. pandas-dev/pandas: Pandas. https://doi.org/10.5281/zenodo.3509134

To, T., Guttmann, A., Dick, P.T., Rosenfield, J.D., Parkin, P.C., Tassoudji, M., Vydykhan, T.N., Cao, H., Harris, J.K., 2004. Risk Markers for Poor Developmental Attainment in Young Children: Results From a Longitudinal National Survey. Arch Pediatr Adolesc Med 158, 643. https://doi.org/10.1001/archpedi.158.7.643

Tokariev, A., Roberts, J.A., Zalesky, A., Zhao, X., Vanhatalo, S., Breakspear, M., Cocchi, L., 2019. Large-scale brain modes reorganize between infant sleep states and carry prognostic information for preterms. Nat Commun 10, 2619. https://doi.org/10.1038/s41467-019-10467-8

Tomchek, S.D., Dunn, W., 2007. Sensory Processing in Children With and Without Autism: A Comparative Study Using the Short Sensory Profile. The American Journal of Occupational Therapy 61, 190–200. https://doi.org/10.5014/ajot.61.2.190

Tooley, U.A., Bassett, D.S., Mackey, A.P., 2021. Environmental influences on the pace of brain development. Nat Rev Neurosci 22, 372–384. https://doi.org/10.1038/s41583-021-00457-5

Torchiano, M., 2020. effsize: Efficient Effect Size Computation. https://doi.org/10.5281/zenodo.1480624

Tzourio-Mazoyer, N., Landeau, B., Papathanassiou, D., Crivello, F., Etard, O., Delcroix, N., Mazoyer, B., Joliot, M., 2002. Automated Anatomical Labeling of Activations in SPM Using a Macroscopic Anatomical Parcellation of the MNI MRI Single-Subject Brain. NeuroImage 15, 273–289. https://doi.org/10.1006/nimg.2001.0978

Van Rossum, G., 2020. The Python Library Reference, release 3.7. Python Software Foundation.

Virtanen, P., Gommers, R., Oliphant, T.E., Haberland, M., Reddy, T., Cournapeau, D., Burovski, E., Peterson, P., Weckesser, W., Bright, J., van der Walt, S.J., Brett, M., Wilson, J., Millman, K.J., Mayorov, N., Nelson, A.R.J., Jones, E., Kern, R., Larson, E., Carey, C.J., Polat, İ., Feng, Y., Moore, E.W., VanderPlas, J., Laxalde, D., Perktold, J., Cimrman, R., Henriksen, I., Quintero, E.A., Harris, C.R., Archibald, A.M., Ribeiro, A.H., Pedregosa, F., van Mulbregt, P.,

SciPy 1.0 Contributors, 2020. SciPy 1.0: Fundamental Algorithms for Scientific Computing in Python. Nature Methods 17, 261–272. https://doi.org/10.1038/s41592-019-0686-2

Vohryzek, J., Deco, G., Cessac, B., Kringelbach, M.L., Cabral, J., 2020. Ghost Attractors in Spontaneous Brain Activity: Recurrent Excursions Into Functionally-Relevant BOLD Phase-Locking States. Frontiers in Systems Neuroscience 14, 1–15. https://doi.org/10.3389/fnsys.2020.00020

Wang, L., Yu, C., Chen, H., Qin, W., He, Y., Fan, F., Zhang, Y., Wang, M., Li, K., Zang, Y., Woodward, T.S., Zhu, C., 2010. Dynamic functional reorganization of the motor execution network after stroke. Brain 133, 1224–1238. https://doi.org/10.1093/brain/awq043

Watanabe, T., Rees, G., 2017. Brain network dynamics in high-functioning individuals with autism. Nature Communications 8, 16048. https://doi.org/10.1038/ncomms16048

Wen, X., Wang, R., Yin, W., Lin, W., Zhang, H., Shen, D., 2020. Development of Dynamic Functional Architecture during Early Infancy. Cerebral Cortex 30, 5626–5638. https://doi.org/10.1093/cercor/bhaa128

Wickham, H., 2021a. tidyr: Tidy Messy Data.

Wickham, H., 2021b. forcats: Tools for Working with Categorical Variables (Factors).

Wickham, H., 2020. modelr: Modelling Functions that Work with the Pipe.

Wickham, H., 2019. stringr: Simple, Consistent Wrappers for Common String Operations.

Wickham, H., 2016. ggplot2: Elegant Graphics for Data Analysis. Springer-Verlag New York.

Wickham, H., François, R., Henry, L., Müller, K., 2021. dplyr: A Grammar of Data Manipulation.

Wildie, M., Shanahan, M., 2012. Metastability and chimera states in modular delay and pulse-coupled oscillator networks. Chaos 22, 043131. https://doi.org/10.1063/1.4766592

Wilke, C.O., 2020a. cowplot: Streamlined Plot Theme and Plot Annotations for "ggplot2."

Wilke, C.O., 2020b. ggtext: Improved Text Rendering Support for "ggplot2."

Xia, M., Wang, J., He, Y., 2013. BrainNet Viewer: A Network Visualization Tool for Human Brain Connectomics. PLoS ONE 8, e68910. https://doi.org/10.1371/journal.pone.0068910

Xie, Y., 2021. knitr: A General-Purpose Package for Dynamic Report Generation in R.

Xie, Y., 2015. Dynamic Documents with R and knitr, 2nd ed. Chapman and Hall/CRC, Boca Raton, Florida.

Xie, Y., 2014. knitr: A Comprehensive Tool for Reproducible Research in R, in: Stodden, V., Leisch, F., Peng, R.D. (Eds.), Implementing Reproducible Computational Research. Chapman and Hall/CRC.

Yu, G., 2021a. shadowtext: Shadow Text Grob and Layer.

Yu, G., 2021b. ggimage: Use Image in "ggplot2."